Title
Small Molecule Inhibition of Rab7 Impairs B Cell Class Switching and Plasma Cell Survival To Dampen the Autoantibody Response in Murine Lupus

Journal
The Journal of Immunology, 197(10)

ISSN
0022-1767

Authors
Lam, Tonika
Kulp, Dennis V
Wang, Rui
et al.

Publication Date
2016-11-15

DOI
10.4049/jimmunol.1601427

Peer reviewed

HHS Public Access

Author manuscript

J Immunol. Author manuscript; available in PMC 2017 November 15.

Published in final edited form as:

J Immunol. 2016 November 15; 197(10): 3792–3805. doi:10.4049/jimmunol.1601427.

Small molecule inhibition of Rab7 impairs B cell class-switching and plasma cell survival to dampen the autoantibody response in murine lupus

Tonika Lam[*,1], **Dennis V. Kulp**[*,1], **Rui Wang**[*,1,2], **Zheng Lou**[*], **Julia Taylor**[*], **Carlos E. Rivera**[*], **Hui Yan**[*], **Qi Zhang**[*], **Zhonghua Wang**[§], **Hong Zan**[*], **Dmitri N. Ivanov**[§], **Guangming Zhong**[*], **Paolo Casali**[*,3], and **Zhenming Xu**[*,3]

[*]Department of Microbiology, Immunology and Molecular Genetics, University of Texas School of Medicine, UT Health Science Center at San Antonio, TX 78229

[§]Department of Biochemistry, University of Texas School of Medicine, UT Health Science Center at San Antonio, TX 78229

Abstract

IgG autoantibodies mediate pathology in systemic lupus patients and lupus-prone mice. Here we showed that the class-switched IgG autoantibody response in MRL/*Fas*$^{lpr/lpr}$ and C57/*Sle1Sle2Sle2* mice was blocked by the CID 1067700 compound, which specifically targeted Rab7, an endosome-localized small GTPase that was upregulated in activated human and mouse lupus B cells, leading to prevention of disease development and extension of life-span. These were associated with decreased IgG-expressing B cells and plasma cells, but unchanged numbers and functions of myeloid cells and T cells. The Rab7 inhibitor suppressed T cell-dependent and T cell-independent antibody responses, but did not affect T cell-mediated clearance of *Chlamydia* infection, consistent with a B cell-specific role of Rab7. Indeed, B cells and plasma cells were inherently sensitive to *Rab7* gene knockout or Rab7 activity inhibition in class-switching and survival, respectively, while proliferation/survival of B cells and generation of plasma cells were not affected. Impairment of NF-κB activation upon Rab7 inhibition, together with the rescue of B cell class-switching and plasma cell survival by enforced NF-κB activation, indicated that Rab7 mediates these processes by promoting NF-κB activation, likely through signal transduction on intracellular membrane structures. Thus, a single Rab7-inhibiting small molecule can target two stages of B cell differentiation to dampen the pathogenic autoantibody response in lupus.

Keywords

Rab7; NF-κB; AID; CSR; plasma cells; autoantibodies; lupus; small molecule compound

Correspondence: Paolo Casali: Phone: (210) 567-3925; Fax: (210) 567-6612; pcasali@uthscsa.edu. Zhenming Xu: Phone: (210) 567-3964; Fax: (210) 567-6612; xuz3@uthscsa.edu.

[1]These authors contributed equally.

[2]Current address: Xiangya School of Medicine, Central South University of China, Changsha, Hunan, China.

[3]These authors jointly directed the study.

Introduction

Class switch DNA recombination (CSR) in the IgH locus substitutes the IgH constant (C_H) region, such as Cμ of IgM expressed in naïve B cells, with Cγ, Cα or Cε, thereby giving rise to IgG, IgA or IgE antibodies. Together with somatic hypermutation (SHM), CSR is central to the maturation of the antibody response to pathogens, as class-switched antibodies display wide tissue distributions and possess diverse biological effector functions (1). These traits also make IgG and IgA autoantibodies highly pathogenic and capable of mediating multiple organ damage in systemic lupus erythematosus (SLE) (2, 3). Un-switched IgM autoantibodies are mostly nonpathogenic and, rather, may mediate frontline immune protection as natural polyreactive antibodies (4). Class-switched B cells further differentiate into memory B cells or plasma cells, which secrete antibodies at a high rate. A hallmark of active lupus is the high number of IgG^+ antibody-secreting cells (ASCs) that produce autoantibodies. These are diverse but generally target nuclear antigens, such as DNA (5, 6), making the mechanisms underlying B cell class-switching and plasma cell generation/maintenance targets of new lupus therapeutics.

Like SHM, CSR requires activation-induced cytidine deaminase (AID, encoded by *AICDA* in humans and *Aicda* in mice). AID expression is mainly restricted in peripheral B cells activated by CD154 engagement of CD40 on the B cell surface or by complex antigens that engage both a Toll-like receptor (TLR) and the B cell receptor (BCR) (7). AID is elevated in B cells of lupus patients and lupus mice, consistent with the heightened CSR/SHM in these B cells (8), and AID deficiency abrogates IgG autoantibodies in lupus-prone MRL/$Fas^{lpr/lpr}$ mice (8, 9). Inhibitors of AID deaminase activity are yet to be developed, thereby emphasizing the need for molecules that target the mechanisms underlying AID induction in order to dampen the class-switched pathogenic autoantibody response.

Rab7 (encoded by *RAB7A* in humans and *Rab7* in mice) is a small GTPase that, when bound to its GTP substrate, promotes endosome maturation and autophagy. As we have shown (10), Rab7 is induced in activated B cells *in vivo* (i.e., in PNA^{hi} germinal center B cells) and *in vitro,* e.g., by CD154 and TLR ligands, the same stimuli that induce AID expression and CSR. It plays a B cell-intrinsic role in antibody responses, as mice that conditionally knockout *Rab7* in activated B cells cannot mount mature antibody responses to T cell-dependent or -independent antigens (10). Rab7 promotes CSR (to IgG, IgE and IgA) and does so by mediating AID induction, as enforced expression of AID rescues CSR in *Rab7* knockout B cells. Further, Rab7 plays an important role in CD40- or TLR-triggered activation of NF-κB, which directly regulates *Aicda* gene transcription by binding to the promoter and enhancers of this gene (1, 11, 12). Rab7 is, however, dispensable for Erk1/Erk2 activation and expression of Blimp-1, both of which critically mediate plasma cell generation (13, 14), and, as a consequence, B cell differentiation into plasma cells, suggesting that Rab7 and its associated intracellular membrane structures (i.e., endosomes) specify receptor-triggered signaling for selective gene expression and B cell differentiation processes (15). Whether Rab7 plays a role in the maintenance of plasma cells remains unclear.

Here we hypothesized that the lupus autoantibody response can be suppressed by inhibition of CSR in B cells and impairment of generation or maintenance of plasma cells, ideally by a single molecule that can target both cell types. To test this hypothesis, we have used a high-affinity and specific Rab7 inhibitor, CID 1067700. This has been identified by high-throughput screening as the only compound to affect the binding of purified recombinant Rab7 to GTP and GDP (16). By analyzing the level of activated Rab7 form (GTP-bound Rab7, Rab7-GTP) in B cells treated with CID 1067700 and using B cell-specific *Rab7* knockout mice as well as retroviruses that enforced specific gene expression, we have verified the specific targeting of Rab7 by this small molecule in B cells and the consequent impairment in NF-κB activation. By using our defined *in vitro* B cell and plasma cell culture systems, we have further analyzed the impact of Rab7 inhibition on B cell class-switching and plasma cell generation/survival as well as the role of Rab7-dependent NF-κB activation in these processes. Finally, by analyzing – for the first time – the *in vivo* effect of the Rab7 inhibition on antibody and autoantibody responses in normal C57BL/6 (C57) mice and two widely used lupus mouse strains, female MRL/$Fas^{lpr/lpr}$ and C57/*Sle1Sle2Sle3* mice (17, 18), we have outlined the potential of Rab7 as a therapeutic target in lupus and possibly other NF-κB-, CSR- and/or plasma cell-mediated disease conditions.

Materials and Methods

Mice, drug treatment, immunization and infection

Female mice were used in all experiments. C57 (Stock # 000664), MRL/$Fas^{lpr/lpr}$ (Stock #000485) and C57/*Sle1Sle2Sle3* (Stock #007228) mice were from The Jackson Laboratory and maintained in a pathogen-free vivarium. Conditional *Rab7* knockout $Igh^{+/C\gamma 1\text{-}cre}Rab7^{fl/fl}$ mice and their "wildtype" $Igh^{+/C\gamma 1\text{-}cre}Rab7^{+/fl}$ littermates on the C57 background were as described (10). $Rosa26^{+/fl\text{-}STOP\text{-}fl\text{-}Ikk\beta ca}$ mice on the C57 background (19) were from The Jackson Laboratory (Stock #008242).

For *in vivo* treatment, CID 1067700 (MLS000673908; SID 24798006; SID 57578339; Glixx Laboratories) dissolved in DMSO (stock concentration 40 mM, 16 mg/ml) was diluted with the solvent to the final volume of 50 μl and injected intraperitoneally (i. p.) once per week at the dose of 16 mg/Kg body weight. This dose was well tolerated by mice at all ages (data not shown); it is within the dose range used in patients and animal models for several drugs with comparable EC_{50} (10–100 nM) to their respective targets (higher doses led to variable mouse death, perhaps due to putative off-targeting effect of the drug). C57, MRL/$Fas^{lpr/lpr}$ and C57/*Sle1Sle2Sle3* mice injected i. p. with the vehicle DMSO (nil; 50 μl) showed no difference in examined parameters, as compared to their respective counterparts without any injection (data not shown). For survival studies and skin lesion analyses, MRL/$Fas^{lpr/lpr}$ mice were treated with nil or CID 1067700 for 10 weeks and maintained until moribund (e.g., showing signs of severe loss of mobility, hunched back, piloerection, ruffled fur, dyspnea, gasping and weight loss), at which point they were euthanized. For other clinical, serological, cellular and molecular analyses (see below), mice were treated for 7 weeks in a "double-blind" manner, as their identities were made unknown to investigators who performed these assays.

For immunization, C57 mice were treated with nil or CID 1067700 7 d before i. p. injection with 100 μg of NP-CGG (in average 16 molecules of 4-hydroxy-3-nitrophenyl acetyl, NP, conjugated to one molecule of chicken γ-globulin; Biosearch Technologies) in 100 μl of alum (Imject® Alum, Pierce) or 25 μg of NP-LPS (0.2 NP molecule conjugated to one LPS molecule; Biosearch Technologies) in 100 μl of PBS. Mice were treated with nil or CID 1067700 once every three days until being sacrificed.

For *Chlamydia muridarum* infection, the Nigg strain was propagated in Hela cells for the isolation of the Nigg3G0.10.1 clone, as previously described (20). Purified Nigg3G0.10.1 elementary bodies (EB) were used to infect 6-week old C57 mice intravaginally with 2×10^5 inclusion-forming units (IFUs). Mice were injected with 2.5 mg of medroxyprogesterone (Depo-Provera; Pharmacia Upjohn) subcutaneously at d −5 to increase the susceptibility and nil or CID 1067700, starting at d −7, once a week for 5 weeks. Mice were monitored for vaginal live organism shedding up to d 63. All protocols were in accordance with rules and regulations of the Institutional Animal Care and Use Committee of the University of Texas Health Science Center at San Antonio (UTHSCSA).

Human and mouse primary B cells

Human PBMCs were prepared, following a standard protocol, from peripheral blood of de-identified SLE patients and healthy subjects, as collected by venipuncture. SLE patients, who were recruited with informed consent under the protocol approved by the Institutional Review Board of UTHSCSA, fulfilled at least four 1982 American Rheumatism Association revised criteria for SLE and had the SLE Disease Activity Index (SLEDAI) above 3. All donors were free of infection by HBV, HCV, HPV, HIV and EBV. To prepare human B cells for stimulation, PBMCs (5×10^7) were subjected to negative selection (against CD2, CD14, CD16, CD27, CD36, CD43 and CD235a) using Human Naïve B Cell Isolation Kit II (Miltenyl) following the manufacturer's instructions, resulting in over 95% IgD^+ B cells (generally over 3×10^6). Cells were analyzed or seeded at 3×10^5 cell/ml for culturing in RPMI 1640 medium (Invitrogen) supplemented with FBS (10% v/v, Hyclone), penicillin-streptomycin/amphotericin B (1% v/v) and 50 μM β-mercaptoethanol (RPMI-FBS).

Mouse immune cells were isolated from single cell suspensions prepared from the spleen and pooled axillary, inguinal and cervical lymph nodes. Lymph node cells were directly lysed for immunoblotting studies. Spleen cells were resuspended in ACK Lysis Buffer (Lonza) to lyse red blood cells and, after quenching with RPMI-FBS, were resuspended in PBS for analysis or further preparation. To isolate B cells, spleen cells were subjected to negative selection (against CD43, CD4, CD8, CD11b, CD49b, CD90.2, Gr-1 or Ter-119) using EasySep™ Mouse B cell Isolation Kit (StemCell™ Technologies) following the manufacturer's instructions, resulting in preparations of more than 98% IgM^+IgD^{hi} B cells. After pelleting, B cells were resuspended in RPMI-FBS before further analysis or stimulation. For cell sorting, spleen cells were stained with fluorophore-labeled anti–CD19 mAb, anti–CD138 mAb, anti–TCR mAb and/or peanut agglutinin (PNA) to purify B cells, activated B cells and plasma cells, as indicated, resulting preparations that were at least 98% pure by post-sorting analysis. Bone marrow cells were isolated form tibia and fibula for myeloid cell differentiation and ELISPOT experiments.

B cell culture, stimulation and drug treatment

Human B cells were stimulated with CD154 (3 U/ml) in the presence of recombinant IL-4 (20 ng/ml; BioLegend) and IL-21 (50 ng/ml; R&D Systems) for 48 h for transcript analyses or 120 h for flow cytometry analysis of class-switched IgG1 and other markers. CD154 was prepared as membrane fragments isolated from Sf21 insect cells infected by CD154-expressing baculovirus, as we described (10, 21) – membrane fragments from non-infected Sf21 cells failed to stimulate B cells. For CSR induction in mouse B cells, spleen B cells were cultured (3×10^5 cell/ml) in RPMI-FBS were stimulated for 96 h (or 48 h for transcript and protein analyses) by the following primary stimuli: CD154 (3 U/ml), LPS (3 μg/ml, from *E. coli*, serotype 055:B5, deproteinized by chloroform extraction; Sigma-Aldrich) or R-848 (30 ng/ml; Invivogen), a ligand of TLR7, which promotes lupus autoantibody responses in a B cell-intrinsic manner. Recombinant IL-4 (4 ng/ml), for CSR to IgG1 and IgE, and TGF-β (2 ng/ml; R&D Systems), for CSR to IgA, and anti–Igδ mAb (clone 11-26c conjugated to dextran, anti–δ/dex, 100 ng/ml; Fina Biosolutions), which crosslinks IgD BCR to potentiate CSR to IgA in primary B cells, were added as indicated. To induce CSR to IgA in the mouse IgM^+ CH12F3 lymphoma cell line, these B cells (10^5 cell/ml) were cultured in RPMI-FBS and stimulated with CD154 (3 U/ml) or, as first shown here, by LPS at low concentrations (100 ng/ml), plus IL-4 and TGF-β for 48 h. To generate plasma cells *in vitro*, purified B cells were stimulated with LPS plus IL-4, TGF-β, anti–Igδ mAb conjugated to dextran (anti–δ/dex) and retinoic acid (RA, 10 μM; Sigma) for 66 h. This condition, as we first found here, resulted in $CD19^{lo}CD138^{hi}$ plasma cells representing over 70% of cells in the culture.

To treat human and mouse B cells *in vitro* with the Rab7 inhibitor, CID 1067700 was diluted in DMSO and added to cell cultures to the final concentration of 40 μM (or as indicated). CID 1067700 or DMSO (nil) was added either at the time when B cell stimulation started, or 66 h after B cells were stimulated with LPS plus IL-4, TGF-β, anti–δ/dex and RA, as indicated, for analysis of plasma cell survival (see below).

Analysis of CSR, cell proliferation and survival—To analyze IgG-expressing B cells and plasma cells *in vivo*, spleen cells (2×10^6) were first stained with fluorophore-labeled mAbs to surface markers and 7–AAD (Supplemental Table 1). After washing, cells were resuspended in the BD Cytofix/Cytoperm™ buffer (250 μl, BD Biosciences) and incubated at 4°C for 20 m. After washing twice with the BD Perm/Wash™ buffer, cells were stained in the same buffer with fluorophore-labeled mAb to IgM, IgG1, IgG2a or IgG2b followed by washing for flow cytometry analysis. Dead ($7–AAD^+$) cells were excluded from analysis. For CSR analysis of B cells stimulated *in vitro*, B cells were analyzed by flow cytometry for surface expression of IgG and IgA as well as intracellular expression of IgE, as we have described (10, 21).

For B cell proliferation analysis *in vivo*, mice were injected i. p. with 2 mg of bromodeoxyuridine (BrdU) in 200 μl PBS twice, with the first and second injection at 24 h and 20 h prior to sacrificing, respectively. Spleen B cells were analyzed for BrdU incorporation (by anti–BrdU mAb staining) and DNA contents (by 7–AAD staining after cells were permeablized) using a BrdU Flow Kit® (BD Biosciences) following the

manufacturer's instructions. For B cell proliferation analysis *in vitro*, naïve B cells were labeled with CFSE (Invitrogen) following the manufacturer's instructions and then cultured for 96 h in the presence of appropriate stimuli. Cells were analyzed by flow cytometry for CFSE intensity, which was reduced by half after completion of each cell division, as CFSE-labeled cell constituents were equally distributed between daughter cells. The number of B cell divisions was determined by the "Proliferation Platform" of the FlowJo® software.

To analyze B cell and plasma cell survival in MRL/$Fas^{lpr/lpr}$ mice treated with CID 1067700 or DMSO *in vivo*, spleen cells were stained with anti–CD19 mAb, anti–CD138 mAb, anti–TCR mAb (to identify $TCR^{-}CD19^{+}CD138^{-}$ B cells and $TCR^{-}CD19^{-/lo}CD138^{+}$ plasma cells) in the presence of mAb Clone 2.4G2, which blocks the FcγIII and FcγII receptors, and 7–AAD without permeabilization (to identify apoptotic/necrotic cells) and analyzed by flow cytometry. To analyze *in vitro* survival of immune cells isolated from MRL/$Fas^{lpr/lpr}$ mice, spleen cells were cultured in RPMI-FBS for 24 or 48 h in the presence of CID 1067700 or DMSO (nil). After staining with surface markers to identify different cell types and 7–AAD, cells were analyzed by flow cytometry. To analyze survival of *in vitro* generated plasma cells (after B cell stimulation with LPS plus IL-4, IL-5, TGF-β, anti–δ/dex and RA for 66 h), cells were washed with RPMI-FBS twice and cultured in RPMI-FBS, without any additional stimuli to block further plasma cell generation, for 24, 48 and 72 h, in the presence of nil or CID 1067700 (40 μM). Cells were collected and stained with mAbs to CD138 and CD19 (to mark plasma cells and B cells) as well as with Annexin V and 7–AAD to distinguish live cells (Annexin $V^{-}7–AAD^{-}$) from cells undergoing early (Annexin $V^{+}7–AAD^{-}$) and late (Annexin $V^{+}7–AAD^{+}$) apoptosis.

Retrovirus transduction

Retroviral vectors pMIG and pMIG-AID (encoding AID) were as described (10); pMIG-Cre (encoding the Cre recombinase) was from Addgene; pMIG-Rab7 and pMIG-Rab2a (encoding Rab7 and Rab2a, respectively) were constructed using specific oligonucleotides (Supplemental Table 2). These vectors were co-transfected with the packaging plasmid into 293T cells to produce retroviruses, as described (10, 22). For transduction, B cells isolated from C57 or $Rosa26^{+/fl\text{-}STOP\text{-}fl\text{-}Ikk\beta ca}$ mice were stimulated with LPS for 24 h in the presence of nil or CID 1067700, as indicated, incubated with viral particles that were pre-mixed with 6 μg/ml DEAE-dextran at 25°C for 30 m (Sigma-Aldrich). After incubation at 37°C for 5 h with gentle mixing every hour, cells were centrifuged at 500 g for 1 h and then 1,000 g for 4 m. Transduced B cells were cultured in virus-free FBS-RPMI in the presence of LPS plus IL-4 for 96 h and then harvested for flow cytometry analysis of expression of GFP (indicating expression of exogenous genes) and IgG1. $Rosa26^{+/fl\text{-}STOP\text{-}fl\text{-}Ikk\beta ca}$ B cells expressed $IKK\beta^{CA}$ (as well as the GFP from the same bi-cistronic transcript) from the *Rosa26* locus upon expression of the Cre recombinase and, consequently, deletion of the "STOP" cassette. Dead ($7–AAD^{+}$) cells were excluded from analysis. To enforce expression of $IKK\beta^{CA}$ in plasma cells pre-generated from B cells stimulated with LPS plus IL-4, TGF-β, anti–δ/dex and RA for 66 h, cells were transduced with pMIG or pMIG-Cre virus, as above, and harvested after 72 h to analyze by flow cytometry the expression of GFP (indicating transduced cells) and plasma cell proportion and viability.

Clinical and pathological analysis of MRL/Fas$^{lpr/lpr}$ mice

Skin lesions, lymphadenopathy and urine protein contents were assessed weekly. Skin lesions were scored on a scale of 0 to 4, with 0 = none, 1 = mild (snout only), 2 = moderate (< 2 cm in snout, ears and back), and 3 = severe (> 2 cm in snout and ears). Lymphadenopathy, as indicated by the appearances of lumps, was scored on a scale of 0 to 4, with 0 = none; 1 = small (at one site), 2 = moderate (at two sites), 3 = large at three or more different sites, and 4 = extremely large (at more than three sites). It was further confirmed by the increase in size of brachial and inguinal lymph nodes when mice were sacrificed. Proteinuria was assessed and scored using semi-quantitative Albustix® strips (Bayer), which, despite giving a range of serum albumin levels for each scale (scale 0 for negative or trace, and 1 through 4), generated few false-positive results when the score was above 3, as observed in virtually all 17-week old MRL/*Fas*$^{lpr/lpr}$ mice. Splenomegaly was assessed when mice were sacrificed by the spleen size.

To assess kidney pathology, kidneys were fixed in Tissue-Tek® OCT™ compound (Sankura Finetek) on dry ice. Seven-μm sections, as prepared by a Cryostat (Leica®), were fixed in cold acetone and stained with FITC-labeled anti–IgG1/anti–IgG2a mAbs. Sections were mounted using ProLong® Gold with DAPI (Invitrogen) for confocal microscopic analysis. For periodic acid–Schiff (PAS) staining, kidneys were fixed in paraformaldehyde (3.6%) at RT for 72 h and, after washing twice with PBS, embedded in paraffin. Five-μm sections were prepared and processed with periodic acid–Schiff (PAS) stain. Glomerular change severity was graded based upon glomerular activity, including glomerular cell proliferation (particularly mesangial matrix expansion), leukocyte infiltration and cellular crescents. Mesangial matrix expansion was grades as follows: 0 = no increase (matrix occupied up to 10% of the glomerulus), 1 = mild (10 – 25%), 2 = moderate (25 – 50%), and 3 = marked (50 – 100%). Leukocyte infiltration is graded as: 1 = mild, 2 = moderate, 3 = extensive. The severity of interstitial mononuclear cell infiltration was based on the ratio of infiltrated areas over the entire section (the value of area was determined by the ImageJ® software), quantified as the average of three sections 200 μM apart, and graded as: 1 = mild, 2 = moderate, 3 = severe.

ELISA, ELISPOT and ANA assays

To determine titers of total IgM, IgG1, IgG2a and IgG2b, sera were first diluted 4 to 128-fold with PBS (pH 7.4) plus 0.05% (v/v) Tween-20 (PBST). Two-fold serially diluted samples and standards for each Ig isotypes were incubated in 96-well plates pre-treated with sodium carbonate/bicarbonate buffer (pH 9.6) and coated with pre-adsorbed goat anti–IgM or anti–IgG (to capture IgG1, IgG2a and IgG2b) Abs (all 1 mg/ml; Supplemental Table 1). After washing with PBST, captured Igs were detected with biotinylated anti–IgM, –IgG1, –IgG2a or –IgG2b Abs (Supplemental Table 1), followed by reaction with horseradish peroxidase (HRP)-labeled streptavidin (Sigma-Aldrich), development with o-phenylenediamine and measurement of absorbance at 492 nm. Ig concentrations were determined using Prism® (GraphPad) or Excel® (Microsoft). To analyze titers of antigen-specific antibodies (high-affinity NP-binding or anti–dsDNA Abs), sera were diluted 1,000-fold in PBST. Twofold serially diluted samples were incubated in a 96-well plate pre-blocked with BSA and coated with NP_4-BSA (in average 4 NP molecules on one BSA

molecule) or dsDNA (10 μg/ml sonicated herring DNA). Captured Igs were detected with biotinylated Ab to IgM, IgG1, IgG2a or IgG3. Data are relative values based on end-point dilution factors.

For ELISPOT analysis of total, NP-binding and dsDNA-binding ASCs, Multi-Screen® filter plates (Millipore) were activated with 35% ethanol, washed with PBS and coated with anti–IgM, anti–IgG, NP_4-BSA or dsDNA (all 5 μg/ml) in PBS. Single spleen or bone marrow cell suspensions were cultured at 50,000 cells/ml in FBS-RPMI supplemented with 50 μM β-mercaptoethanol at 37°C for 16 h. After supernatants were removed, plates were incubated with biotinylated goat anti–mouse IgM, –IgG1, –IgG2a or –IgG3 Ab, as indicated, for 2 h and, after washing, incubated with HRP-conjugated streptavidin. Plates were developed using the Vectastain AEC peroxidase substrate kit (Vector Laboratories). The stained area in each well was quantified using the CTL Immunospot software (Cellular Technology) and depicted as the percentage of total area of each well for ASC quantification.

For semi-quantitative ANA assays of sera from MRL/*Fas*$^{lpr/lpr}$ and C57/*Sle1Sle2Sle3* mice, sera were serially diluted in PBS (from 1:40 to 1:160), incubated on antinuclear Ab substrate slides (HEp-2 cell-coated slides, MBL-BION) and detected with a 1:1 mixture of FITC-labeled anti–IgG1 and anti–IgG2a mAbs (Supplemental Table 1) following manufacturer's instructions. Images were acquired with an Olympus CKX41 fluorescence microscope.

Cytokine intracellular staining

Spleen cells were cultured in RPMI-FBS and stimulated with phorbol 12-myristate 13-acetate (PMA, 20 ng/ml) plus ionomycin (1 μg/ml; both from BioLegend) for 4 h at 37°C in the presence of brefeldin A (BFA). After pelleting, cells were stained with anti–CD4 mAb and Fixable Viability Dye eFluo®450 (FVD eFluo®450) followed by incubation with the BD Cytofix/Cytoperm™ buffer at 4°C for 20 m. After washing twice with the BD Perm/Wash™ buffer, cells were resuspended in Hank's Buffered Salt Solution (HBSS) with 1% BSA and stored overnight at 4°C. Cells were then stained with anti–IFN-γ and anti–IL-17 mAbs conjugated to different fluorophores in Perm/Wash™ buffer and analyzed by flow cytometry. Dead (FVD eFluo® 450$^+$) cells were excluded.

Myeloid cell differentiation and function

Bone marrow cells (10^7) were cultured for 10 d in RPMI-FBS in the presence of conditioned media from L-929 cells that express macrophage colony-stimulating factor (M-CSF, which promotes differentiation into CD11b$^+$ macrophages) or recombinant murine Flt3-ligand (which promotes differentiation into CD11c$^+$ DCs, Peprotech), resulting in generation of over 90% of CD11b$^+$ or 20% of CD11c$^+$ cells. After stimulation with TLR9 ligand CpG ODN for 1 h, cells were collected for RNA extraction and transcript analysis.

GST-RILP pull-down

RILP is an effector protein of activated Rab7 (Rab7-GTP). The *E. coli* strain BL21 harboring GST or GST-RILP expressing vector, as previously described (23), was grown at 37°C to an O.D. of 0.6 before induced by isopropyl-1-thio-β-D-galactopyranoside (IPTG, 0.5 mM) at 30°C for 4 h to express GST or GST-RILP. After pelleting and washing with

cold PBS, bacterial cells were resuspended in 5 ml of cold lysis buffer (25 mM Tris-HCl pH 7.4, 1 M NaCl, 0.5 mM EDTA, 1 mM dithiothreitol and 0.1% Triton X-100) supplemented with a protease inhibitor cocktail (Sigma) and sonicated. Lysates were cleared and, after 5 ml of cold lysis buffer was added, incubated with 300 μl of pre-equilibrated slurry (50% packed volume) of glutathione-Sepharose 4B beads (GE Healthcare) at RT for 30 m. After washing with lysis buffer, beads (30 μl) with immobilized GST or GST-RILP were resuspended as slurry for protein quantification by the Bradford assay and pre-equilibrated in pull-down buffer (20 mM HEPES, 100 mM NaCl, 5 mM $MgCl_2$ and 1% Triton X-100 plus protease inhibitor cocktail). Beads were then incubated by rotating with lysates (300 μg) prepared from stimulated B cells in the pull-down buffer at 4°C overnight. After washing twice with cold pull-down buffer, bound proteins were eluted by incubation of beads in the SDS-PAGE sample buffer at 95°C for 10 m. Immobilized GST-RILP was analyzed by SDS-PAGE/immunoblotting using anti–GST mAb; Rab7-GTP was analyzed by immunoblotting using anti–Rab7 mAb.

Purification of recombinant Rab7 and NMR spectroscopy analysis

DNA sequence encoding Rab7 (human RAB7A amino acid residues 2 – 207) was synthesized using codon optimization for *E.coli* expression and cloned into the pET30a vector, which allows for expression of an N-terminal Strep-tag followed by a SUMO tag. After plasmid transformation, BL21(DE3) cells were grown at 37°C in minimum media until the culture OD_{600} reached 0.6. After the culture was transferred to 18°C, protein expression was induced by IPTG (1 mM) for 15 h. For protein purification, lysates were first subjected to streptactin affinity chromatography and then removal of the Strep-SUMO tag by digestion of SUMO protease at 4°C overnight, resulting in release of cleaved Rab7 (with an additional N-terminal Thr residue) into the supernatants. Trace amounts of cleaved tag were removed by a new round of strep-tactin affinity chromatography. Protein purity was > 90%.

For NMR spectroscopy analysis of free RAB7A, RAB7A (0.3 mM) was exchanged into the buffer containing 20 mM NaPO4 (20 mM, pH 6.9), NaCl (100 mM) and TCEP (1 mM). with 10% D_2O. 2D ^{1}H-^{15}N HSQC was acquired with 2048 and 128 complex points in the direct and indirect dimensions, respectively. For acquisition of the NMR spectrum of RAB7A in complex with CID 1067700, 2.5 μl of CID 1067700 stock solution (40 mM in DMSO) was added to 40 μl of RAB7A to yield final 1:8 protein:compound ratio, followed by NMR spectrum acquisition using the same parameters.

Docking analysis

All modeling studies were performed using the Schrodinger 2015-3 software suite and its graphical interface, Maestro. The crystal structure of the GTP-bound Rab7 (PDBID: 1T91) was used as the docking target for CID 1067700. The bound GTP molecule and all water molecules were removed from the structure prior to docking. Docking was performed with Glide using first standard precision protocol to identify all possible poses with favorable Glide scores.

Chlamydia titration

For monitoring live organism shedding from swab samples, vaginal/cervical swabs were taken at the time points, as indicated. Each swab was soaked in 0.5 ml of sucrose-phosphate-glutamic acid (SPG) and vortexed with glass beads to release chlamydial organisms into supernatants. IFUs were titrated on HeLa cell monolayers in duplicates. The infected cultures were processed for immunofluorescence assays. Briefly, inclusions were counted in five random fields per coverslip under a fluorescence microscope. For coverslips with less than one IFU per view field, IFUs on entire coverslips were counted. Coverslips showing obvious cytotoxicity of HeLa cells were excluded. The total number of IFUs was calculated based on the mean IFUs per view, the ratio of the view area to that of the well, the dilution factor and inoculation volumes.

Flow cytometry, immunoblotting, cDNA synthesis and quantitative RT-PCR (qRT-PCR)

These methods were as we previously described (7, 10, 22). Antibodies (Supplemental Table 1) and oligonucleotides (Supplemental Table 2) used had been validated to be specific. Flow cytometry data were analyzed using the FlowJo® software (Tree Star). For immunoblotting, signals were quantified by Image J (NIH). For qRT-PCR, the ΔΔCt method was used to determine levels of transcripts and data were normalized to levels of *CD79B* (human) or *Cd79b* (mouse), which encodes the BCR Igβ chain that is constitutively expressed in B cells and, to a lesser degree, plasma cells.

Statistical analysis

Most statistical analyses were performed by one-tailed type 1 (for pairwise comparison) or type 2 student t-test. Survival data were analyzed by the Mantel-Cox log-rank test. *Chlamydia* infection data were analyzed by the Wilcoxon rank sum test. *P* values less than 0.05 were considered significant.

More Materials and Methods in Supplemental Materials

Results

Rab7 is highly expressed in human and mouse lupus B cells

Rab7 is upregulated in normal B cells by CSR-inducing stimuli (10), prompting us to analyze its expression in B cells from SLE patients and lupus mice. Peripheral blood mononuclear cells (PBMCs) from SLE patients expressed higher levels of *RAB7A* and *AICDA* transcripts than healthy subjects (Fig. 1A). Likewise, B cells, including PNA^{hi} B cells, from lupus-prone MRL/$Fas^{lpr/lpr}$ and C57/*Sle1Sle2Sle3* mice displayed elevated *Rab7* and *Aicda* transcripts as compared to those from age-matched C57 counterparts (Fig. 1B, 1C). A similar difference was observed in Rab7 and AID protein levels in lymphoid organs (Fig. 1D). Thus, lupus B cells dysregulate Rab7 expression.

Targeting of Rab7 by CID 1067700 inhibits NF-κB activation and AID induction in B cells

In view of treating lupus-prone mice with Rab7 inhibitor CID 1067700, we first tested the ability of this small molecule to inhibit CSR *in vitro.* CID 1067700 treatment of mouse B cells stimulated by CD154 or LPS plus IL-4 impaired Rab7 activation, as shown by reduced

Rab7-GTP levels in RILP pull-down assays but normal Rab7 expression (Fig. 2A, 2B). This led to reduced AID expression and CSR to IgG1, despite normal B cell proliferation and germline I_H-C_H transcription, both of which are required for CSR (Fig. 2B–2D). Consistent with the requirement of AID for CSR to all Ig isotypes, CID 1067700 inhibited induction of CSR to IgG, IgA and IgE in human and mouse B cells (Fig. 2E–2H).

CID 1067700 binds Rab7 with a high affinity (EC_{50}: 10-20 nM), but was also shown to bind several small GTPases with much lower affinity (i.e., with EC_{50} being at least 80 nM) and could affect functions of these GTPases in cell lines (16, 24). In our hands, it directly bound purified recombinant Rab7 (Fig. 3A), likely through two binding sites on the surface of Rab7, as suggested by computational docking of CID 1067700 onto the crystal structure of Rab7, with one site overlapping with the GTP binding site and the other located on the opposite face (Fig. 3B). In stimulated primary B cells, which upregulate Rab7 expression, CID 1067700 specifically targeted Rab7, as its inhibitory activity was abrogated when *Rab7* was ablated in $Igh^{+/C\gamma 1\text{-}cre}Rab7^{fl/fl}$ conditional knockout B cells (Fig. 3C) – these knockout B cells showed reduced CSR (10). Conversely, CSR in CID 1067700-treated B cells was rescued by enforced expression of Rab7, but not Rab2a, a putative off-target of CID 1067700 (Fig. 3D). It was also increased by AID, which could rescue CSR in *Rab7* knockout B cells (10).

Like *Rab7* deficiency, inhibition of Rab7 activity by CID 1067700 resulted in defective canonical NF-κB activation and normal non-canonical NF-κB activation (Fig. 2B). Expression of $IKK\beta^{CA}$, a constitutively active mutant of IKKβ that can lead to canonical NF-κB hyperactivation (19) restored CSR in CID 1067700-treated B cells (Fig. 3E), indicating that the major defect in these cells is the impairment of canonical NF-κB activation.

Thus, specific Rab7 inhibition in B cells hampers NF-κB activation, AID expression and CSR induction without affecting B cell proliferation.

CID 1067700 blunts pathogenic autoantibody responses in lupus mice

The Rab7 upregulation in lupus B cells, together with the role of Rab7 in NF-κB activation, AID expression and CSR, all of which are also elevated in lupus B cells and implicated in lupus pathogenesis (25, 26), suggested that Rab7 inhibition would hamper NF-κB-dependent pathogenic autoantibody responses *in vivo*, e.g., in MRL/$Fas^{lpr/lpr}$ mice. These mice developed malar rash and dorsal skin lesions, lymphadenopathy, splenomegaly and nephritis, leading to mortality as early as at 11-week of age and an average life-span of about 20 weeks, with more than half of mice moribund between 17- and 23-week of age (Fig. 4A, 4B). When treated with CID 1067700 for only 10 weeks (starting at 10-week, one week before appearance of the first dead mouse in the untreated cohort), 14 of 16 MRL/$Fas^{lpr/lpr}$ mice survived past the treatment period and half of mice were alive at 52 weeks, compared to only one in the untreated cohort (Fig. 4A). Treated mice had normal body weight, rare skin lesions and reduced lymphadenopathy and splenomegaly at 17 weeks (Fig. 4B–4D). They had some interstitial infiltration by monocytes (likely myeloid cells and T cells), but were largely free of glomerulonephritis, showing little proteinuria and decreased

"crescent" formation and mesangial matrix expansion in glomeruli (Fig. 4E, 4F and not shown).

Lupus nephritis is tightly associated with and/or caused by deposition of immunocomplexes (ICs) that contain class-switched IgG autoantibodies in the kidney. IgG-IC deposition was reduced in MRL/*Fas*$^{lpr/lpr}$ mice treated with CID 1067700 (Fig. 5A). Serum levels of IgG anti-nuclear antibodies (ANAs) were also decreased in treated MRL/*Fas*$^{lpr/lpr}$ and C57/*Sle1Sle2Sle3* mice (Fig. 5B). As shown by time-course analyses of autoantibodies that bound double-strand DNA (anti–dsDNA), the ratio of pathogenic IgG classes, e.g., IgG1, IgG2a and IgG2b, over the non-pathogenic IgM class (IgG/IgM, depicted as R^{IgG}) remained low in treated mice despite variations of IgG and IgM titers in different mice in the same cohort (Fig. 5C and data not shown). So did R^{IgG} for total IgG, in contrast to the steadily increased anti–dsDNA and total R^{IgG}, until peaking, in untreated mice (Fig. 5C). Thus, inhibition of Rab7 suppresses IgG autoantibody responses and prevents development of disease symptoms in lupus mice, leading to significantly increased life-span.

CID 1067700 targets B cells and specifically impairs the CSR machinery in vivo

The reduction of R^{IgG} suggested that the CSR process was inhibited in CID 1067700-treated MRL/*Fas*$^{lpr/lpr}$ mice. Indeed, these mice showed unchanged number of B cells but significantly decreased IgG$^+$ B cells, concomitant with a slightly increased proportion of un-switched IgM$^+$ B cells (Fig. 6A). Decreased CSR, as also shown by reduced post-recombination Iμ-Cγ transcripts (the molecular indicators of completed CSR), was associated with lower expression of CSR machinery genes, such as *Aicda* and *14-3-3*γ, which is important for the targeting of AID to IgH switch (S) regions and is induced in an NF-κB-dependent manner (22, 27, 28); *Rab7* expression was also slightly reduced (Fig. 6B). Expression of the *A20* (*Tnfaip3*) gene, which dampens NF-κB activation and controls autoimmunity (29), or germline Iμ-Cμ transcription, however, was not affected; neither was expression of *Prdm1* (encoding Blimp-1), *Xbp1*, which is essential for the plasma cell secretion function, or genes (*Vps34, LC3* and *Becn1*) implicated in autophagy, which regulates plasma cell differentiation/functions (30, 31). Treated B cells were normal in proliferation, CD21/CD35 expression, induction of the CD80 activation markers and expression of CD40 and MHC II, which are important for B cells to interact with CD4$^+$ T helper cells (Fig. 6C), thereby emphasizing the inherent nature of the CSR machinery defect.

Rab7 has been suggested to be expressed in myeloid cells, in addition to B cells (32), prompting us to analyze the impact of Rab7 inhibition on CD11b$^+$ macrophages and CD11c$^+$ dendritic cells (DCs). The proportions of these cells, their survival *in vitro* and induced expression of cytokines that could influence B cells and autoantibody responses, such as BAFF and type I interferon (IFNα and IFNβ), were not affected by CID 1067700 treatment in MRL/*Fas*$^{lpr/lpr}$ mice, with the only exception of reduced *Il1b* expression in CD11c$^+$ DCs (Fig. 7A–7C). Reflecting the low expression of Rab7 in T cells and a modest role of this molecule in T cell functions (33), CID 067700 treatment did not change the proportions of total CD4$^+$ T cells and those producing IFN-γ, which is critical for CSR to IgG2a and important in systemic autoimmunity (34–36), in MRL/*Fas*$^{lpr/lpr}$ mice or survival of CD4$^+$ lupus T cells *in vitro* (Fig. 7C, 7D). This, together with the ability of CID 1067700-

treated C57 mice to clear *Chlamydia* infection, which is dependent on T cells, but not B cells or plasma cells (37, 38), showed that this small molecule does not have a major impact on T cells (Fig. 7E). Thus, CID 1067700 selectively targets B cells and impairs the CSR machinery in lupus-prone mice without altering proliferation/activation of B cells.

Rab7 deficiency or Rab7 inhibition reduces ASCs

Consistent with the surge of IgG^+ ASCs during lupus flare, most cells expressing the plasma cell marker CD138 in MRL/*Fas*$^{lpr/lpr}$ mice with active lupus (e.g., at 17-week) were IgG^+, as shown by intracellular staining (Fig. 8A). Upon Rab7 inhibition, IgG^+ plasma cells were greatly decreased (due to defective CSR) with a concomitant increase in the proportion of IgM^+ plasma cells. However, the number of ASCs that produced IgM autoantibodies (e.g., anti–dsDNA) remained unchanged (Fig. 8B). This together with the lower number of $IgG1^+$ and $IgG2a^+$ ASCs indicated an overall reduction in ASCs upon treatment with CID 1067700. This Rab7 inhibitor had similar effect on ASCs in C57 mice, as indicated by the reduced antigen-specific $IgG1^+$ ASCs and unchanged IgM^+ ASCs in the spleen of mice injected with a T-dependent (NP-CGG) or T-independent (NP-LPS) antigen, which resulted in virtual abrogation of circulating antigen-specific IgGs (Fig. 8C). Likewise, *Rab7* knockout in B cells and their plasma cell progenies, as occurring in *Igh*$^{+/C\gamma 1\text{-}cre}$*Rab7*$^{fl/fl}$ mice, reduced total and antigen-specific $IgG1^+$ ASCs (our previous findings, (10)) with no increase in IgM^+ ASCs (Fig. 8D). ASCs in the bone marrow, in which long-lived plasma cells take residence (39), were even more sensitive to Rab7 inhibition or knockout, as both IgG^+ and IgM^+ ASCs were decreased (Fig. 8C, 8D). Finally, IgG^+ ASCs preformed *in vivo* were vulnerable to CID 1067700 treatment, as they failed to produce antibodies *ex vivo* (Fig. 8E). Thus, abrogation of Rab7 expression or inhibition of its activity in normal and lupus-prone mice affects ASC production/maintenance, thereby compounding the defect in CSR to suppress class-switched antibody and autoantibody responses.

Rab7 inhibition impairs plasma cell survival

Despite their impact on ASCs (consisting of plasmablasts and plasma cells), neither CID 1067700 nor *Rab7* knockout affected *in vitro* generation of $CD138^{hi}$ cells upon induction of B cells by all tested stimuli, such as LPS plus IL-4, TGF-β, BCR crosslinking and retinoic acid (RA), which led to more than 70% of live cells being $CD138^{hi}$ (Fig. 9A and not shown). This suggested that Rab7 was not involved in plasma cell generation and prompted us to analyze the effect of CID 1067700 on plasma cell survival. In MRL/*Fas*$^{lpr/lpr}$ mice, CID 1067700 treatment resulted in increased death and reduced number of $CD138^{hi}$ cells (Fig. 9B, 9C). Even residual live $CD138^{hi}$ cells expressed lower levels of *Cxcr4, Il6r* and *Vla4*, all of which encode surface receptors that mediate plasma cell survival – by contrast, expression of *Bcma* and *Taci*, which are important for APRIL-dependent survival, was not affected (Fig. 9D). Expression of intracellular factors important for plasma cell survival (such as *Irf4, Mcl1,* and *Hdac11*) as well as the *Atg5* autophagy gene was also affected. Expression of *Prdm1* or *Xbp1*, which are important to maintain the plasma cell secretory function but dispensable for their survival (40), however, was not affected. To further confirm that Rab7 inhibition directly affects plasma cell survival, we treated $CD138^{hi}$ cells generated *in vitro* with CID 1067700. These cells displayed high levels of early and late apoptosis, as compared to the much slower loss of viability in their untreated counterparts (Fig. 9E).

Enforced NF-κB activation through IKKβ^{CA} expression prevented CD138^{hi} cells from being killed by CID 1067700 (Fig. 9F), showing that Rab7 plays a role in the plasma cell survival *in vivo* and *in vitro*, in part by mediating NF-κB-activation.

Discussion

Stemming from our previous findings (10), data reported here have further outlined an important role of Rab7 in antibody and autoantibody responses, owing to its functions in modulating *Aicda* expression, B cell class-switching and plasma cell survival. In spite of the partial impairments of these processes by Rab7 inhibition or knockout, their combined outcome was the virtual abrogation of class-switched specific antibodies in normal mice and paucity of pathogenic autoantibodies in lupus-prone mice. As we showed, small molecule Rab7 inhibition hampered CSR induced by all primary stimuli, including the one (CD154) produced by T cells, which mediate many autoimmune conditions in part by dysregulating B cells, and a ligand (R-848) of TLR7, an endosomal TLR that strongly promotes lupus pathogenesis and does so in a B cell-intrinsic manner (41). Thus, Rab7, which is an endosome-tethered protein, participates in B lineage cell differentiation processes initiated by many immune receptors irrespective of their initial locations, e.g., CD40 and TLR4 on the surface and TLR7 in the endosome. Surface immune receptors, however, need to be internalized for Rab7 to mediate CSR and plasma cell survival, likely in a manner dependent on Rab7^{+} endosomes.

As indicated by our results showing IKKβ^{CA}-mediated rescue of CSR and plasma cell survival in CID 1067700-treated cells, the B cell- and plasma cell-intrinsic roles of Rab7 are, at least in part, through activation of NF-κB, a transcription factor central to B lineage cell functions (42, 43). Rab7-dependent NF-κB activation, however, is dispensable for B cell development and differentiation into plasma cells, as suggested by unchanged numbers of CD19^{+} B cells in CID 1067700-treated mice *in vivo* and generation of plasma cells from CID 1067700-treated B cells or *Rab7* knockout B cells *in vitro*. It would also be absent during early activation of naïve B cells upon CD40 or TLR engagement, as these cells express low levels of Rab7 and contain sparse intracellular membrane structures. Only after Rab7 upregulation, likely together with expansion of the intracellular membrane network, would Rab7 nucleate the assembly of putative “intracellular signalosomes” on different membrane types (e.g., endosomes in B cells and autophagosomes in plasma cells) – through mechanisms that are not yet clear – for sustained NF-κB activation. This would be required for efficient AID induction in CSR, which takes at least 48 h to unfold, and continuous expression of genes in plasma cells to maintain survival. By contrast, Rab7-independent early NF-κB activation would occur through different signalosomes, e.g., those on the plasma membrane in B cells with cell surface receptor engagement. It also plays a role in the *Rab7* gene transcription, possibly through several κB sites in the promoter region (unpublished data).

Rab7 is inherently the preferred target of CID 1067700, as shown by its much lower EC_{50} as compared to the few small GTPase off-targets of this compound (16). As suggested by our docking analyses, CID 1067700 could potentially bind at two distinct sites on the Rab7 surface. Existence of a candidate binding site that is different from the GTP-binding site (the

site that also exists in potential off-targets of CID 1067700) would, at least in part, explain the Rab7-specific inhibitory activity of CID 1067700. This together with upregulated Rab7 expression in B cells (and likely in plasma cells), including in PNA^{hi} germinal center B cells in immunized mice, would underpin the specific inhibition of Rab7 by CID 1067700, as more molecules would be available for targeting. Likewise, the dysregulated Rab7 expression would make lupus B cells preferred targets of CID 1067700. Such dysregulation may be the consequence of a putative positive-feedback loop involving NF-κB hyperactivation (25, 26). It could also be exacerbated by female hormones, as suggested by enhancement of Rab7 expression by estrogens (our unpublished data). This together with estrogen upregulation of AID expression through the HoxC4 homeodomain transcription factor would contribute to the female bias of autoantibody-mediated systemic autoimmunity (11, 44, 45). In the subset of human lupus B cells that displayed moderate Rab7 expression, as shown in our studies, NF-κB hyperactivation may be through alternative mechanisms, such as A20 downregulation (29).

Rab7 inhibition reduced expression of several genes instrumental to plasma cell survival, such as *Cxcr4*, *Irf4* and *Mcl1* (40, 46, 47). Expression of CXCR4 (a G protein-coupled receptor) has been shown to be boosted by NF-κB, consistent with the identification of several κB sites in the *Cxcr4* gene locus (48), consistent with a role of Rab7 in NF-κB activation and rescue of survival of CID 1067700-treated plasma cells with enforced expression of $IKK\beta^{CA}$. The presence of several Irf4-binding sites in the *Cxcr4* promoter (49) also suggests that *Cxcr4* transcription is regulated by Irf4, whose expression would be mediated by Rab7 (shown here) and promoted by NF-κB (50). Expression of *Mcl1* in plasma cells is in general lower than that in B cells (51), perhaps explaining higher sensitivity of plasma cells to death upon Rab7 inhibition. Rab7 deficiency or inhibition in mice may also impair the autophagy-dependent antibody secretion, which together with decreased plasma cell survival would lead to marked reduction in ASCs. Like anti–dsDNA-specific ASCs in the spleen, kidney resident plasma cells that secret pathogenic nephrophilic antibodies (52–54) may be reduced, leading to significantly reduced kidney damage.

As a small molecule, CID 1067700 injected i. p. was “metabolized” *in vivo* and required weekly administration to maintain detectable levels in the circulation and lymphoid organs (our unpublished observations). Despite this, Rab7 inhibition by CID 1067700 could prevent development of lupus pathology in MRL/$Fas^{lpr/lpr}$ mice and extend the lifespan by more than 32 weeks, after a treatment period of only 10 weeks, suggesting that long-lasting changes had occurred in treated B cells – treated plasma cells would die. These changes likely include alterations in the epigenome in lupus B cells with extended survival (due to the *Fas/lpr* mutation) as well as changes in the BCR repertoire and/or the memory autoreactive B cell compartment. Putative epigenetic changes might occur through downregulation of NF-κB-dependent expression of histone modifying enzymes and/or re-balance of exaggerated Rab7-dependent autophagy, which modulates the microRNA machinery (15, 55). B cell-intrinsic mechanisms may be further complemented by changes in regulatory immune elements, such as T regulatory cells and DCs (56), possibly including altered type-I IFN gene signatures in plasmacytoid DCs (pDCs), as short-term pDC ablation could also elicit long-term prevention of nephritis in the BXSB lupus mouse mode (57). Such DC changes, however, would be indirect, as CID 1067700 did not decrease cytokine production

by DCs *in vitro*. High Rab7 expression levels in DCs, however, do suggest that Rab7 regulate certain DC functions, perhaps antigen/autoantigen presentation through autophagy induction (58) and MyD88 signaling, which mediates skin lesions (59). By contrast, Rab7 is largely dispensable for T cell survival and functions (e.g., in clearing primary *Chlamydia* infection, as shown here). Addressing specific roles of Rab7 in these and other immune compartments requires generation of different conditional knockout mice.

In contrast to the non-discriminating B cell-depletion lupus therapeutics approaches, CID 1067700 or its future derivatives with improved pharmacodynamics and pharmacokinetics properties would maintain IgM^+ B cells and protective IgMs. It is conceivable that a Rab7 inhibitor can be combined with anti–BAFF or anti–CD20 mAb towards better therapeutic effects (60–62). Such an inhibitor may also be combined with a histone deacetylase (HDAC) inhibitor (HDI) to abrogate plasma cells by affecting plasma cell survival and generation, respectively – synthetic and naturally occurring (e.g., butyrate, a metabolite of gut microbiota) HDIs blunt antibody and autoantibody responses by inhibiting CSR/SHM and B cell differentiation into plasma cells, but not plasma cell survival (3, 21). The translational implications of Rab7-dependent NF-κB activation extend beyond lupus. Rab7 may promote B cell lymphomagenesis mediated by NF-κB hyperactivation (63–65), as suggested by the frequent DNA insertions/deletions and chromosomal translocations in/around the human *RAB7A* locus on the chromosome 3 (3q21) in hematologic malignancies (66–68). It may also play a role in NF-κB-mediated survival of multiple myelomas (69), as it does in maintaining the survival of plasma cells. Addressing these possibilities would greatly expand our studies towards the understanding of the role of Rab7 in immune regulation.

Supplementary Material

Refer to Web version on PubMed Central for supplementary material.

Acknowledgments

This work was supported by National Institutes of Health (NIH) grants AI 079705 and AI 105813 (to P. C.), AI 124172 (to Z. X.), AI 104476 (to D. N. I.) and AI 047997 (to G. Z.). P. C. was also partially supported by the Alliance for Lupus Research (ALR) Target Identification in Lupus Grant ALR 295955 and the Zachry Foundation Distinguished Chair, D. N. I. by a Voelcker Fund Young Investigator Award, H. Z. by an Arthritis National Research Foundation research grant and R. W. by the Xiangya School of Medicine, Central South University of China.

We thank Crystal Lafleur for technical help, Tian Shen for help in plasma cell induction, Egest J. Pone and Christie-Lynn Mortales for ELISPOT, Tamara McRae for PAS kidney histology analysis, Dr. Dmytro Kovalskyy for docking analyses, Dr. Benjamin J. Daniel and Karla M. Gorena in the UTHSCSA Flow Core Facility for help with cell sorting, and the UTHSCSA NMR and Analytical Ultracentrifugation Core Facility (supported in part by the NIH P30 CA054174 to the Cancer Therapy and Research Center of UTHSCSA) for NMR analysis. We thank Dr. Aimee L. Edinger for the RILP-expressing construct, Dr. Nu Zhang for help with cytokine intracellular staining and Dr. Xiaodong Li for help with myeloid cell differentiation assays.

Abbreviations used

AID	activation-induced cytidine deaminase
ASC	antibody-secreting cell
CSR	class switch DNA recombination

Rab7	Ras-related in brain7
SLE	systemic lupus erythematosus

References

1. Xu Z, Zan H, Pone EJ, Mai T, Casali P. Immunoglobulin class-switch DNA recombination: induction, targeting and beyond. Nat Rev Immunol. 2012; 12:517–531. [PubMed: 22728528]
2. Tsokos GC. Systemic lupus erythematosus. N Engl J Med. 2011; 365:2110–2121. [PubMed: 22129255]
3. Zan H, Casali P. Epigenetics of peripheral B-cell differentiation and the antibody response. Front Immunol. 2015; 6:631. [PubMed: 26697022]
4. Elkon K, Casali P. Nature and functions of autoantibodies. Nat Clin Pract Rheumatol. 2008; 4:491–498. [PubMed: 18756274]
5. Venkatesh J, Yoshifuji H, Kawabata D, Chinnasamy P, Stanevsky A, Grimaldi CM, Cohen-Solal J, Diamond B. Antigen is required for maturation and activation of pathogenic anti-DNA antibodies and systemic inflammation. J Immunol. 2011; 186:5304–5312. [PubMed: 21444762]
6. Tipton CM, Fucile CF, Darce J, Chida A, Ichikawa T, Gregoretti I, Schieferl S, Hom J, Jenks S, Feldman RJ, Mehr R, Wei C, Lee FE, Cheung WC, Rosenberg AF, Sanz I. Diversity, cellular origin and autoreactivity of antibody-secreting cell population expansions in acute systemic lupus erythematosus. Nat Immunol. 2015; 16:755–765. [PubMed: 26006014]
7. Pone EJ, Zhang J, Mai T, White CA, Li G, Sakakura JK, Patel PJ, Al-Qahtani A, Zan H, Xu Z, Casali P. BCR-signalling synergizes with TLR-signalling for induction of AID and immunoglobulin classswitching through the non-canonical NF-kappaB pathway. Nat Commun. 2012; 3:767. [PubMed: 22473011]
8. Zan H, Zhang J, Ardeshna S, Xu Z, Park SR, Casali P. Lupus-prone MRL/faslpr/lpr mice display increased AID expression and extensive DNA lesions, comprising deletions and insertions, in the immunoglobulin locus: concurrent upregulation of somatic hypermutation and class switch DNA recombination. Autoimmunity. 2009; 42:89–103. [PubMed: 19156553]
9. Jiang C, Foley J, Clayton N, Kissling G, Jokinen M, Herbert R, Diaz M. Abrogation of lupus nephritis in activation-induced deaminase-deficient MRL/lpr mice. J Immunol. 2007; 178:7422–7431. [PubMed: 17513793]
10. Pone EJ, Lam T, Lou Z, Wang R, Chen Y, Liu D, Edinger AL, Xu Z, Casali P. B cell Rab7 mediates induction of activation-induced cytidine deaminase expression and class-switching in T-dependent and T-independent antibody responses. J Immunol. 2015; 194:3065–3078. [PubMed: 25740947]
11. Park SR, Zan H, Pal Z, Zhang J, Al-Qahtani A, Pone EJ, Xu Z, Mai T, Casali P. HoxC4 binds to the promoter of the cytidine deaminase AID gene to induce AID expression, class-switch DNA recombination and somatic hypermutation. Nat Immunol. 2009; 10:540–550. [PubMed: 19363484]
12. Tran TH, Nakata M, Suzuki K, Begum NA, Shinkura R, Fagarasan S, Honjo T, Nagaoka H. B cell-specific and stimulation-responsive enhancers derepress Aicda by overcoming the effects of silencers. Nat Immunol. 2010; 11:148–154. [PubMed: 19966806]
13. Nutt SL, Hodgkin PD, Tarlinton DM, Corcoran LM. The generation of antibody-secreting plasma cells. Nat Rev Immunol. 2015; 15:160–171. [PubMed: 25698678]
14. Minnich M, Tagoh H, Bonelt P, Axelsson E, Fischer M, Cebolla B, Tarakhovsky A, Nutt SL, Jaritz M, Busslinger M. Multifunctional role of the transcription factor Blimp-1 in coordinating plasma cell differentiation. Nat Immunol. 2016; 17:331–343. [PubMed: 26779602]
15. Lou Z, Casali P, Xu Z. Regulation of B cell differentiation by intracellular membrane-associated proteins and microRNAs: role in the antibody response. Front Immunol. 2015; 6:537. [PubMed: 26579118]
16. Agola JO, Hong L, Surviladze Z, Ursu O, Waller A, Strouse JJ, Simpson DS, Schroeder CE, Oprea TI, Golden JE, Aube J, Buranda T, Sklar LA, Wandinger-Ness A. A competitive nucleotide binding inhibitor: in vitro characterization of Rab7 GTPase inhibition. ACS Chem Biol. 2012; 7:1095–1108. [PubMed: 22486388]

17. Perry D, Sang A, Yin Y, Zheng YY, Morel L. Murine models of systemic lupus erythematosus. J Biomed Biotechnol. 2011; 2011:271694. [PubMed: 21403825]
18. Mohan C. The long (and sometimes endless) road to murine lupus genes. J Immunol. 2015; 195:4043–4046. [PubMed: 26477046]
19. Sasaki Y, Derudder E, Hobeika E, Pelanda R, Reth M, Rajewsky K, Schmidt-Supprian M. Canonical NF-kappaB activity, dispensable for B cell development, replaces BAFF-receptor signals and promotes B cell proliferation upon activation. Immunity. 2006; 24:729–739. [PubMed: 16782029]
20. Zhang Q, Huang Y, Gong S, Yang Z, Sun X, Schenken R, Zhong G. In vivo and ex vivo imaging reveals a long-lasting Chlamydial infection in the mouse gastrointestinal tract following genital tract inoculation. Infect Immun. 2015; 83:3568–3577. [PubMed: 26099591]
21. White CA, Pone EJ, Lam T, Tat C, Hayama KL, Li G, Zan H, Casali P. Histone deacetylase inhibitors upregulate B cell microRNAs that silence AID and Blimp-1 expression for epigenetic modulation of antibody and autoantibody responses. J Immunol. 2014; 193:5933–5950. [PubMed: 25392531]
22. Li G, White CA, Lam T, Pone EJ, Tran DC, Hayama KL, Zan H, Xu Z, Casali P. Combinatorial H3K9acS10ph histone modification in IgH locus S regions targets 14-3-3 adaptors and AID to specify antibody class-switch DNA recombination. Cell Rep. 2013; 5:702–714. [PubMed: 24209747]
23. Romero Rosales K, Peralta ER, Guenther GG, Wong SY, Edinger AL. Rab7 activation by growth factor withdrawal contributes to the induction of apoptosis. Mol Biol Cell. 2009; 20:2831–2840. [PubMed: 19386765]
24. Hong L, Guo Y, BasuRay S, Agola JO, Romero E, Simpson DS, Schroeder CE, Simons P, Waller A, Garcia M, Carter M, Ursu O, Gouveia K, Golden JE, Aube J, Wandinger-Ness A, Sklar LA. A Pan-GTPase inhibitor as a molecular probe. PLoS One. 2015; 10:e0134317. [PubMed: 26247207]
25. Zhang W, Shi Q, Xu X, Chen H, Lin W, Zhang F, Zeng X, Zhang X, Ba D, He W. Aberrant CD40-induced NF-kappaB activation in human lupus B lymphocytes. PLoS One. 2012; 7:e41644. [PubMed: 22952582]
26. Zubair A, Frieri M. NF-kappaB and systemic lupus erythematosus: examining the link. J Nephrol. 2013; 26:953–959. [PubMed: 23807646]
27. Xu Z, Fulop Z, Wu G, Pone EJ, Zhang J, Mai T, Thomas LM, Al-Qahtani A, White CA, Park SR, Steinacker P, Li Z, Yates J 3rd, Herron B, Otto M, Zan H, Fu H, Casali P. 14-3-3 adaptor proteins recruit AID to 5′-AGCT-3′-rich switch regions for class switch recombination. Nat Struct Mol Biol. 2010; 17:1124–1135. [PubMed: 20729863]
28. Mai T, Pone EJ, Li G, Lam TS, Moehlman J, Xu Z, Casali P. Induction of activation-induced cytidine deaminase-targeting adaptor 14-3-3gamma is mediated by NF-kappaB-dependent recruitment of CFP1 to the 5′-CpG-3′-rich 14-3-3gamma promoter and is sustained by E2A. J Immunol. 2013; 191:1895–1906. [PubMed: 23851690]
29. Ma A, Malynn BA. A20: linking a complex regulator of ubiquitylation to immunity and human disease. Nat Rev Immunol. 2012; 12:774–785. [PubMed: 23059429]
30. Pengo N, Scolari M, Oliva L, Milan E, Mainoldi F, Raimondi A, Fagioli C, Merlini A, Mariani E, Pasqualetto E, Orfanelli U, Ponzoni M, Sitia R, Casola S, Cenci S. Plasma cells require autophagy for sustainable immunoglobulin production. Nat Immunol. 2013; 14:298–305. [PubMed: 23354484]
31. Conway KL, Kuballa P, Khor B, Zhang M, Shi HN, Virgin HW, Xavier RJ. ATG5 regulates plasma cell differentiation. Autophagy. 2013; 9:528–537. [PubMed: 23327930]
32. Shay T, Kang J. Immunological Genome Project and systems immunology. Trends Immunol. 2013; 34:602–609. [PubMed: 23631936]
33. Roy SG, Stevens MW, So L, Edinger AL. Reciprocal effects of rab7 deletion in activated and neglected T cells. Autophagy. 2013; 9:1009–1023. [PubMed: 23615463]
34. Theofilopoulos AN, Koundouris S, Kono DH, Lawson BR. The role of IFN-gamma in systemic lupus erythematosus: a challenge to the Th1/Th2 paradigm in autoimmunity. Arthritis Res. 2001; 3:136–141. [PubMed: 11299053]

35. Domeier PP, Chodisetti SB, Soni C, Schell SL, Elias MJ, Wong EB, Cooper TK, Kitamura D, Rahman ZS. IFN-γ receptor and STAT1 signaling in B cells are central to spontaneous germinal center formation and autoimmunity. J Exp Med. 2016; 213doi: 10.1084/jem.20151722
36. Jackson SW, Jacobs HM, Arkatkar T, Dam EM, Scharping NE, Kolhatkar NS, Hou B, Buckner JH, Rawlings DJ. B cell IFN-γ receptor signaling promotes autoimmune germinal centers via cell-intrinsic induction of BCL-6. J Exp Med. 2016; 213doi: 10.1084/jem.20151724
37. Morrison RP, Caldwell HD. Immunity to murine chlamydial genital infection. Infect Immun. 2002; 70:2741–2751. [PubMed: 12010958]
38. Morrison SG, Su H, Caldwell HD, Morrison RP. Immunity to murine Chlamydia trachomatis genital tract reinfection involves B cells and CD4(+) T cells but not CD8(+) T cells. Infect Immun. 2000; 68:6979–6987. [PubMed: 11083822]
39. Chernova I, Jones DD, Wilmore JR, Bortnick A, Yucel M, Hershberg U, Allman D. Lasting antibody responses are mediated by a combination of newly formed and established bone marrow plasma cells drawn from clonally distinct precursors. J Immunol. 2014; 193:4971–4979. [PubMed: 25326027]
40. Tellierm J, Shi W, Minnich M, Laio Y, Crawford S, Smyth GK, Kallies A, Busslinger M, Nutt SL. Blimp-1 controls plasma cell function through the regulation of immunoglobulin secretion and the unfolded protein response. Nat Immunol. 2016; 17:323–330. [PubMed: 26779600]
41. Walsh ER, Pisitkun P, Voynova E, Deane JA, Scott BL, Caspi RR, Bolland S. Dual signaling by innate and adaptive immune receptors is required for TLR7-induced B-cell-mediated autoimmunity. Proc Natl Acad Sci USA. 2012; 109:16276–16281. [PubMed: 22988104]
42. Baltimore D. NF-kappaB is 25. Nat Immunol. 2011; 12:683–685. [PubMed: 21772275]
43. Heise N, De Silva NS, Silva K, Carette A, Simonetti G, Pasparakis M, Klein U. Germinal center B cell maintenance and differentiation are controlled by distinct NF-kappaB transcription factor subunits. J Exp Med. 2014; 211:2103–2118. [PubMed: 25180063]
44. Mai T, Zan H, Zhang J, Hawkins JS, Xu Z, Casali P. Estrogen receptors bind to and activate the HOXC4/HoxC4 promoter to potentiate HoxC4-mediated activation-induced cytosine deaminase induction, immunoglobulin class switch DNA recombination, and somatic hypermutation. J Biol Chem. 2010; 285:37797–37810. [PubMed: 20855884]
45. White CA, Seth Hawkins J, Pone EJ, Yu ES, Al-Qahtani A, Mai T, Zan H, Casali P. AID dysregulation in lupus-prone MRL/Fas(lpr/lpr) mice increases class switch DNA recombination and promotes interchromosomal c-Myc/IgH loci translocations: modulation by HoxC4. Autoimmunity. 2011; 44:585–598. [PubMed: 21585311]
46. O'Connor BP, Gleeson MW, Noelle RJ, Erickson LD. The rise and fall of long-lived humoral immunity: terminal differentiation of plasma cells in health and disease. Immunol Rev. 2003; 194:61–76. [PubMed: 12846808]
47. Peperzak V, Vikstrom I, Walker J, Glaser SP, LePage M, Coquery CM, Erickson LD, Fairfax K, Mackay F, Strasser A, Nutt SL, Tarlinton DM. Mcl-1 is essential for the survival of plasma cells. Nat Immunol. 2013; 14:290–297. [PubMed: 23377201]
48. Helbig G, Christopherson KW 2nd, Bhat-Nakshatri P, Kumar S, Kishimoto H, Miller KD, Broxmeyer HE, Nakshatri H. NF-kappaB promotes breast cancer cell migration and metastasis by inducing the expression of the chemokine receptor CXCR4. J Biol Chem. 2003; 278:21631–21638. [PubMed: 12690099]
49. Liu X, Chen X, Zhong B, Wang A, Wang X, Chu F, Nurieva RI, Yan X, Chen P, van der Flier LG, Nakatsukasa H, Neelapu SS, Chen W, Clevers H, Tian Q, Qi H, Wei L, Dong C. Transcription factor achaete-scute homologue 2 initiates follicular T-helper-cell development. Nature. 2014; 507:513–518. [PubMed: 24463518]
50. Grumont RJ, Gerondakis S. Rel induces interferon regulatory factor 4 (IRF-4) expression in lymphocytes: modulation of interferon-regulated gene expression by rel/nuclear factor kappaB. J Exp Med. 2000; 191:1281–1292. [PubMed: 10770796]
51. Luckey CJ, Bhattacharya D, Goldrath AW, Weissman IL, Benoist C, Mathis D. Memory T and memory B cells share a transcriptional program of self-renewal with long-term hematopoietic stem cells. Proc Natl Acad Sci USA. 2006; 103:3304–3309. [PubMed: 16492737]

52. Sekine H, Watanabe H, Gilkeson GS. Enrichment of anti-glomerular antigen antibody-producing cells in the kidneys of MRL/MpJ-Fas(lpr) mice. J Immunol. 2004; 172:3913–3921. [PubMed: 15004199]
53. Starke C, Frey S, Wellmann U, Urbonaviciute V, Herrmann M, Amann K, Schett G, Winkler T, Voll RE. High frequency of autoantibody-secreting cells and long-lived plasma cells within inflamed kidneys of NZB/W F1 lupus mice. Eur J Immunol. 2011; 41:2107–2112. [PubMed: 21484784]
54. Mohan C, Putterman C. Genetics and pathogenesis of systemic lupus erythematosus and lupus nephritis. Nat Rev Nephrol. 2015; 11:329–341. [PubMed: 25825084]
55. Li G, Zan H, Xu Z, Casali P. Epigenetics of the antibody response. Trends Immunol. 2013; 34:460–470. [PubMed: 23643790]
56. Son M, Kim SJ, Diamond B. SLE-associated risk factors affect DC function. Immunol Rev. 2016; 269:100–117. [PubMed: 26683148]
57. Rowland SL, Riggs JM, Gilfillan S, Bugatti M, Vermi W, Kolbeck R, Unanue ER, Sanjuan MA, Colonna M. Early, transient depletion of plasmacytoid dendritic cells ameliorates autoimmunity in a lupus model. J Exp Med. 2014; 211:1977–1991. [PubMed: 25180065]
58. Deretic V, Saitoh T, Akira S. Autophagy in infection, inflammation and immunity. Nat Rev Immunol. 2013; 13:722–737. [PubMed: 24064518]
59. Teichmann LL, Schenten D, Medzhitov R, Kashgarian M, Shlomchik MJ. Signals via the adaptor MyD88 in B cells and DCs make distinct and synergistic contributions to immune activation and tissue damage in lupus. Immunity. 2013; 38:528–540. [PubMed: 23499488]
60. La Cava A. Targeting the BLyS-APRIL signaling pathway in SLE. Clin Immunol. 2013; 148:322–327. [PubMed: 23269199]
61. Hahn BH. Belimumab for systemic lupus erythematosus. N Engl J Med. 2013; 368:1528–1535. [PubMed: 23594005]
62. Wang W, Rangel-Moreno J, Owen T, Barnard J, Nevarez S, Ichikawa HT, Anolik JH. Long-term B cell depletion in murine lupus eliminates autoantibody-secreting cells and is associated with alterations in the kidney plasma cell niche. J Immunol. 2014; 192:3011–3020. [PubMed: 24574498]
63. Calado DP, Zhang B, Srinivasan L, Sasaki Y, Seagal J, Unitt C, Rodig S, Kutok J, Tarakhovsky A, Schmidt-Supprian M, Rajewsky K. Constitutive canonical NF-kappaB activation cooperates with disruption of BLIMP1 in the pathogenesis of activated B cell-like diffuse large cell lymphoma. Cancer Cell. 2010; 18:580–589. [PubMed: 21156282]
64. Staudt LM. Oncogenic activation of NF-kappaB. Cold Spring Harb Perspect Biol. 2010; 2:a000109. 000110.001101/cshperspect.a000109. [PubMed: 20516126]
65. Zhang B, Calado DP, Wang Z, Frohler S, Kochert K, Qian Y, Koralov SB, Schmidt-Supprian M, Sasaki Y, Unitt C, Rodig S, Chen W, Dalla-Favera R, Alt FW, Pasqualucci L, Rajewsky K. An oncogenic role for alternative NF-kappaB signaling in DLBCL revealed upon deregulated BCL6 expression. Cell Rep. 2015; 11:715–726. [PubMed: 25921526]
66. Kashuba VI, Gizatullin RZ, Protopopov AI, Allikmets R, Korolev S, Li J, Boldog F, Tory K, Zabarovska V, Marcsek Z, Sumegi J, Klein G, Zabarovsky ER, Kisselev L. NotI linking/jumping clones of human chromosome 3: mapping of the TFRC, RAB7 and HAUSP genes to regions rearranged in leukemia and deleted in solid tumors. FEBS Lett. 1997; 419:181–185. [PubMed: 9428630]
67. Mitelman F, Mertens F, Johansson B. A breakpoint map of recurrent chromosomal rearrangements in human neoplasia. Nat Genet. 1997; 15(Spec No):417–474. [PubMed: 9140409]
68. Wieser R, Schreiner U, Pirc-Danoewinata H, Aytekin M, Schmidt HH, Rieder H, Fonatsch C. Interphase fluorescence in situ hybridization assay for the detection of 3q21 rearrangements in myeloid malignancies. Genes Chrom Cancer. 2001; 32:373–380. [PubMed: 11746978]
69. Ni H, Ergin M, Huang Q, Qin JZ, Amin HM, Martinez RL, Saeed S, Barton K, Alkan S. Analysis of expression of nuclear factor kappa B (NF-kappa B) in multiple myeloma: downregulation of NF-kappa B induces apoptosis. Br J Haematol. 2001; 115:279–286. [PubMed: 11703322]
70. Amarilyo G, Lourenco EV, Shi FD, La Cava A. IL-17 promotes murine lupus. J Immunol. 2014; 193:540–543. [PubMed: 24920843]

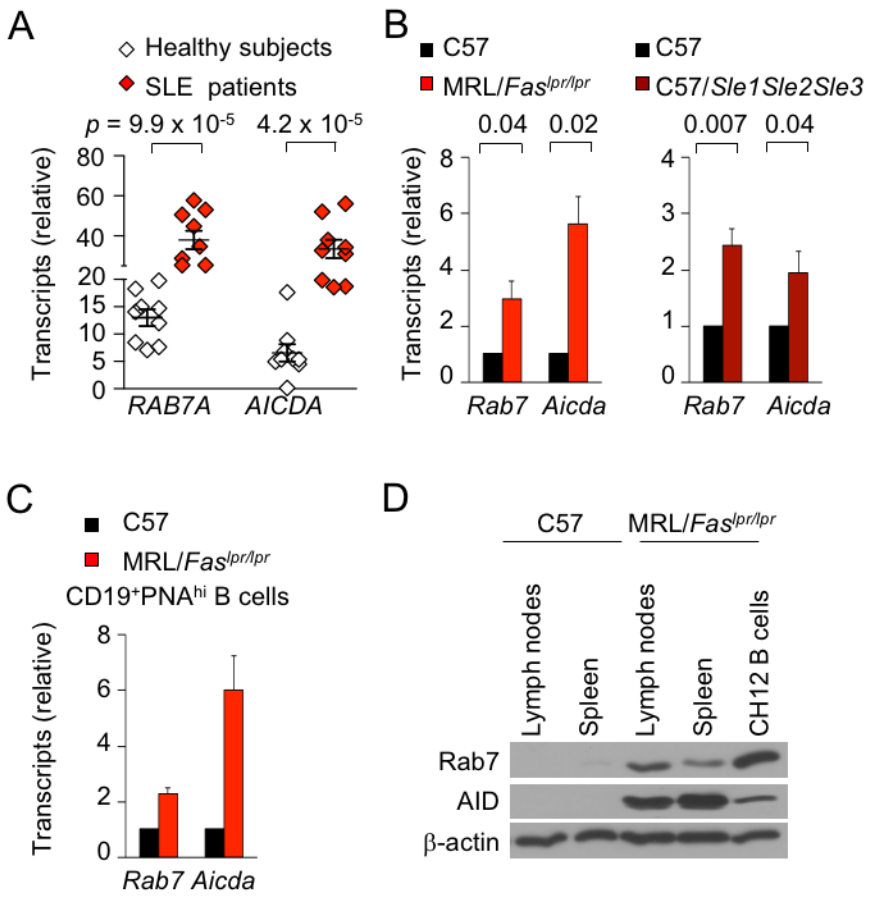

FIGURE 1.

Rab7 is highly expressed in human and mouse lupus B cells. (**A**) qRT-PCR analysis of levels of *RAB7A* and *AICDA* transcripts in PBMCs isolated from lupus patients or healthy subjects (n = 9). Expression of *RAB7B*, which is unrelated to *RAB7A* and is not evolutionarily conserved, was comparable in these samples (data not shown). (**B**) qRT-PCR analysis of *Rab7* and *Aicda* transcripts in spleen B cells isolated from 10-week old MRL/*Fas*$^{lpr/lpr}$ mice and 36-week old C57/*Sle1/Sle2/Sle3* mice. Data are expressed as ratios of values to those in B cells from age-matched C57 mice (mean and s.d. of data from three independent experiments). (**C**) qRT-PCR analysis of *Rab7* and *Aicda* transcripts in sorted spleen CD19^{+}PNA^{hi} cells (>95% pure, which displayed higher Rab7 expression than CD19^{+}PNA^{lo} cells, not shown) from 10-week MRL/*Fas*$^{lpr/lpr}$ mice and NP-CGG-immunized C57 mice. Representative of two independent experiments (mean and s.e.m. of triplicate samples). (**D**) Immunoblotting analysis of Rab7 and AID in spleen and lymph node cells isolated from 10-week old MRL/*Fas*$^{lpr/lpr}$ and C57 mice as well as CH12 B cells.

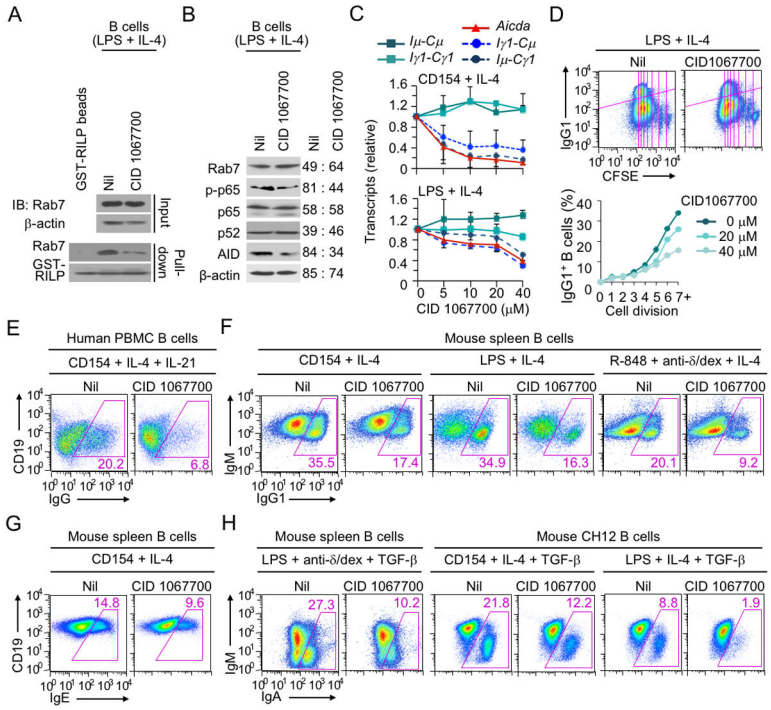

FIGURE 2.

CID 1067700 inhibits Rab7 activity, NF-κB activation, AID expression and CSR in B cells. (**A**) GST-RILP pull-down analysis of Rab7-GTP (bottom panels) in B cells stimulated with LPS plus IL-4 for 48 h in the presence of nil or CID 1067700. Expression of total Rab7 was also analyzed (top panels). (**B**) Immunoblotting of Rab7, phosphorylated and total p65 in the canonical NF-κB pathway, p52 in the non-canonical NF-κB activation pathway, AID and β-actin in stimulated B cells treated with nil or CID 1067700. Numbers on the right side indicate non-normalized values of quantified signals. (**C**) qRT-PCR analysis of levels of IgH germline Iμ-Cμ and Iγ1-Cγ1 transcripts, *Aicda*, post-recombination Iμ-Cγ1 and circle Iγ1-Cμ transcript in B cells stimulated with CD154 or LPS plus IL-4 and treated with different doses of CID 1067700. Data are expressed as ratios of values in CID 1067700-treated B cells to those in untreated cells (mean and s.e.m. of data from triplicate samples). (**D**) Flow cytometry analysis of proliferation and CSR to IgG1 in CFSE-labeled B cells after stimulation in the presence of nil or CID 1067700 (top panels) and depiction of the proportion of switched $IgG1^+$ cells in B cells that had completed each cell division (bottom panels). (**E–H**) CSR to different Ig isotypes in human or mouse B cells stimulated by different combinations of a T-dependent or T-independent primary CSR-inducing stimulus and a secondary inducing stimulus, as indicated, in the presence of nil or CID 1067700. (**A, B, E–H**), representative of three independent experiments.

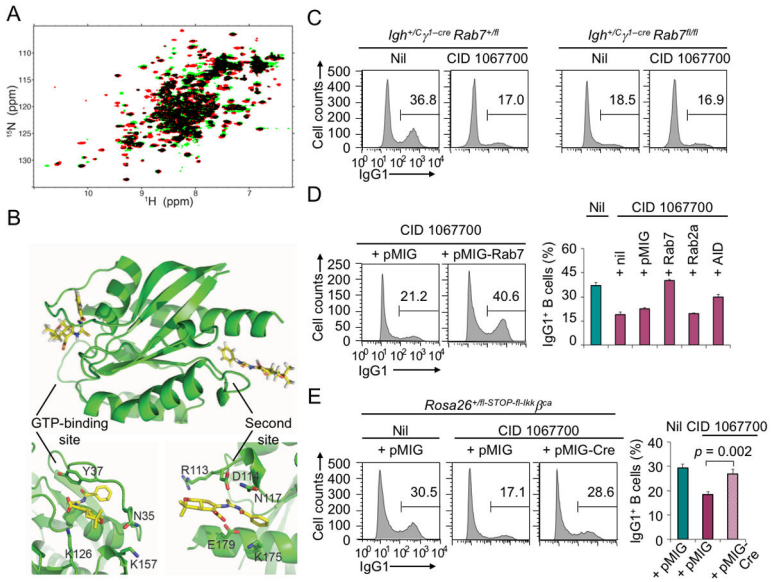

FIGURE 3.

CID 1067700 inhibit CSR in B cells by targeting Rab7. (**A**) NMR spectroscopy analysis of direct physical interaction of CID 1067700 with Rab7. Spectra of free Rab7 and Rab7:CID 1067700 were represented by red and green signals, respectively, with overlapping signals shown in black. Chemical shift perturbations and broadening observed for NMR signals (non-overlapping signals) of multiple Rab7 residues are indicative of direct physical interaction. (**B**) Docking analysis of two candidate CID 1067700 binding sites on the opposite faces of Rab7 (left panel). The more favorable docking score (Glide score –5.5) was obtained for CID 1067700 binding at the GTP-binding site of Rab7 (lower left panel) and the second binding site (Glide score –2.7) located on the opposite face of Rab7 when CID 1067700 adopts a different conformation (lower right panel). The interaction interface within the GTP-binding site was slightly different from that predicted by others (16). (**C**) Flow cytometry analysis of CSR to IgG1 in B cells from *Igh*$^{+/C\gamma 1\text{-}cre}$*Rab7*$^{+/fl}$ and *Igh*$^{+/C\gamma 1\text{-}cre}$*Rab7*$^{fl/fl}$ littermates after stimulation with LPS plus IL-4 in the presence of nil or CID 1067700. Representative of three independent experiments. (**D**) CSR to IgG1 in B cells pre-stimulated with LPS in the presence of CID 1067700, transduced with pMIG or pMIG-Rab7 and then stimulated with LPS plus IL-4 for 72 h (left panels). The histogram (right panel) depicts CSR rescue by Rab7, Rab2a, a potential off-target of CID 1067700 with EC_{50} (170 nM) much higher than Rab7 (10-20 nM), or AID. Other potential off-targets (http://tinyurl.com/obgvd3v) are three small GTPases with EC_{50} comparable to Rab2a (i.e., H-Ras, 20-145 nM; Rac1, 80 nM; and Cdc42, 91-129 nM), much weaker targets (i.e., autophagy protein ATG4B, EC_{50} of 13 μM, and histone lysine methyltransferase G9a, EC_{50} of 39 μM), and growth factors/receptors (i.e., FGF22, GFER, VLA-4 and EGFR) that have not been independently verified as potential off-targets and, to our best knowledge, are not known to regulate CSR (mean and s.e.m. of three independent experiments). (**E**) CSR to IgG1 in B cells isolated from *Rosa26*$^{+/fl\text{-}STOP\text{-}fl\text{-}Ikk\beta ca}$ mice and transduced with pMIG or pMIG-*Cre* (which encoded the Cre recombinase to delete the “STOP” cassette in the *Rosa26* locus and,

therefore, allow for expression of IKKβ^{CA}) and then stimulated with LPS plus IL-4 in the presence of nil or CID 1067700 (mean and s.e.m. of four experiments).

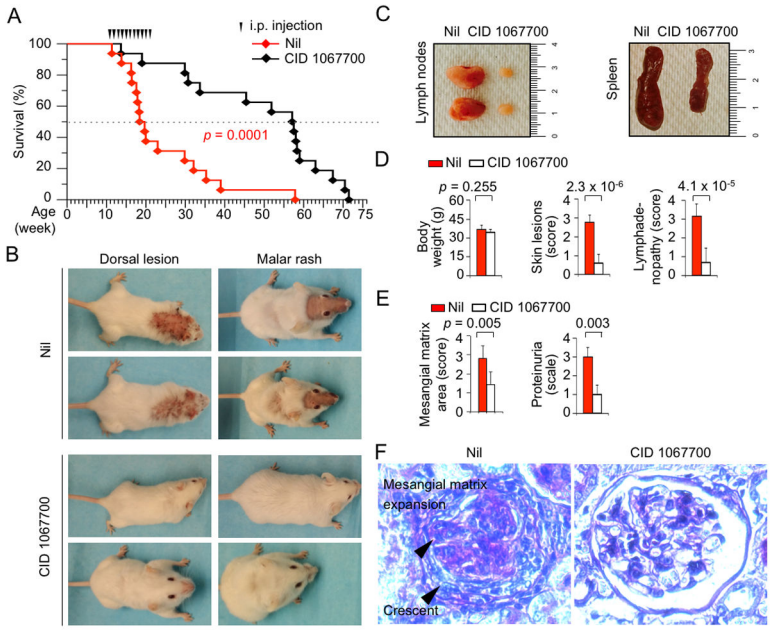

FIGURE 4.

Rab7 inhibition by CID 1067700 prevents disease development in lupus-prone mice. (**A**) Survival curve of 16 MRL/*Fas*$^{lpr/lpr}$ mice treated with nil or CID 1067700. The survival of mice maintained in our facility was similar to that reported by The Jackson Laboratory and other groups. (**B**) Skin lesions in 26-week old nil-or CID 1067700-treated MRL/*Fas*$^{lpr/lpr}$ mice. (**C–F**) Spleens and cervical lymph nodes (**C**), physiological metrics as indicated (**D**), indices of kidney damages (**E**) and PAS staining of kidney sections (**F**) in 17-week old MRL/*Fas*$^{lpr/lpr}$ mice treated with nil or CID 1067700 (**C** and **F**, representative of three independent experiments; **D** and **E**, mean and s.d. of four pairs).

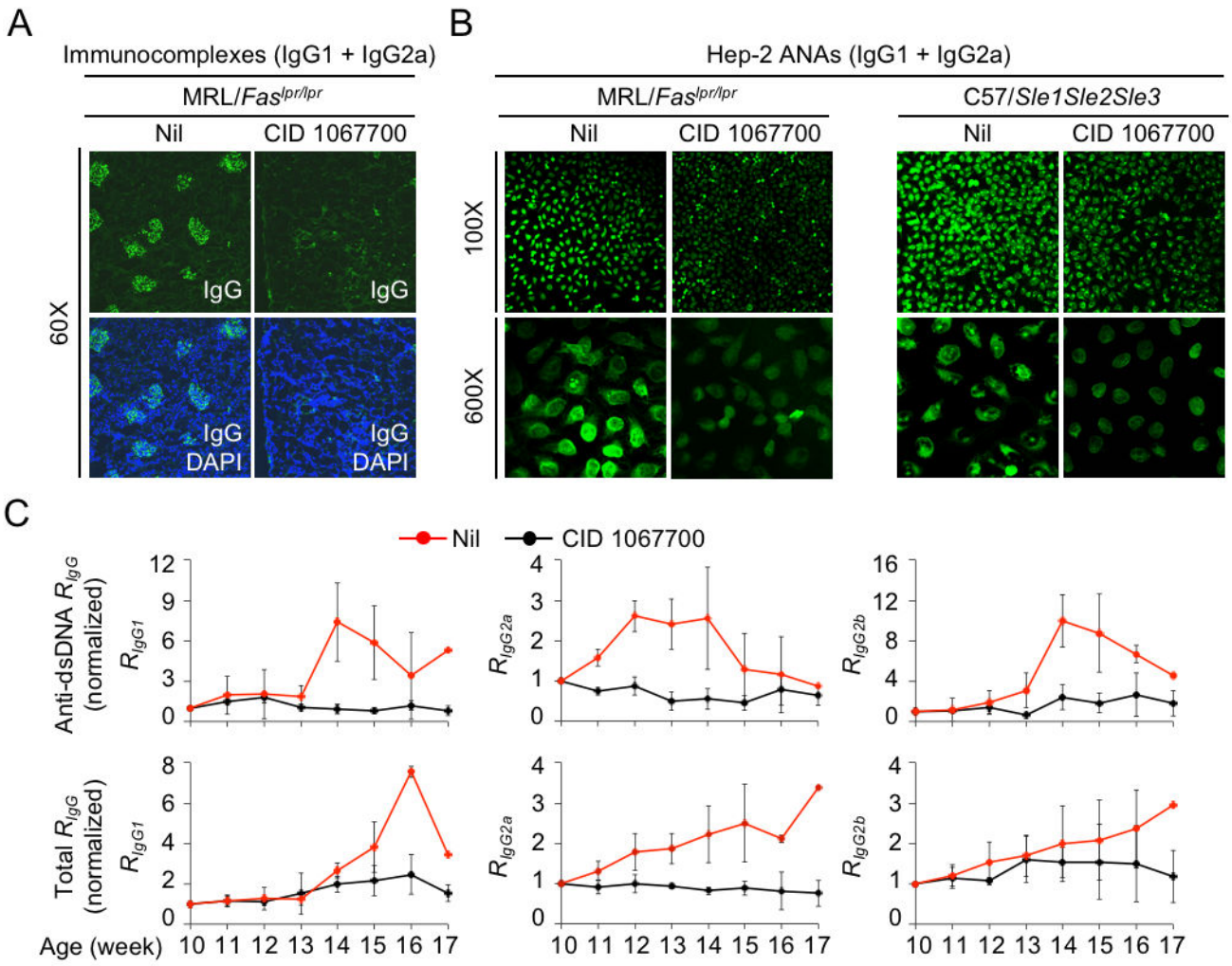

FIGURE 5.

Rab7 inhibition blocks generation of pathogenic autoantibodies. (**A**) IgG-IC formation in the kidney 17-week nil- or CID 1067700-treated MRL/*Fas*$^{lpr/lpr}$ mice (representative of kidney sections in three independent experiments). (**B**) ANA levels in serum samples (diluted 40-fold) from MRL/*Fas*$^{lpr/lpr}$ mice, as in (**A**), and 54-week old nil- or CID 1067700-treated C57/*Sle1Sle2Sle3* mice. ANAs to different autoantigens, as shown by different patterns of fluorescence images at higher magnifications, were all reduced in CID 1067700-treated mice (representative of three independent experiments). More diluted serum samples, e.g., by 160-fold, from CID 1067700-treated mice showed virtually no signals (not shown). (**C**) Ratios of anti–dsDNA (top panels) and total (bottom panels) IgG1, IgG2a and IgG2b titers to titers of the IgM counterparts in nil- or CID 1067700-treated MRL/*Fas*$^{lpr/lpr}$ mice at different ages, as indicated. Data were normalized to values in mice at the age of from 10-week (set as 1), right before the treatment started, and were depicted as *RIgG1, RIgG2a* and *RIgG2b* (mean and s.e.m. of four mice per group). IgG3 titers were generally low (not shown).

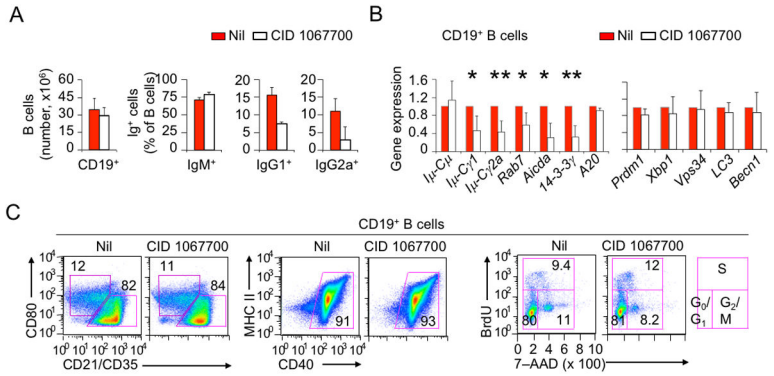

FIGURE 6.

Rab7 inhibition hampers CSR in lupus-prone mice. (**A**) Flow cytometry analysis of number of B cells (left panel) and proportion of IgM^+, $IgG1^+$ and $IgG2a^+$ cells among B cells (right panels) in 17-week old nil- or CID 1067700-treated MRL/*Fas*$^{lpr/lpr}$ mice (mean and s.d. of four pairs of mice) – the proportion of these B cells was increased due to the reduced splenomegaly (data not shown). Both nil- and CID 1067700-treated MRL/*Fas*$^{lpr/lpr}$ mice had B lymphocytopenia, with average of 3.2×10^7 $CD19^+$ B cells per spleen, as compared to about 5.5×10^7 B cells in age-matched C57 mice (data not shown). Moribund MRL/*Fas*$^{lpr/lpr}$ mice were excluded from analyses due to their severe B lymphocytopenia. (**B**) Expression of different transcripts, as indicated, in $CD19^+$ B cells sorted from MRL/*Fas*$^{lpr/lpr}$ mice, as in (**A**). Data were depicted as the ratio of values in CID 1067700-treated mice to those in nil-treated mice (*, $p < 0.05$; **, $p < 0.01$). (**C**) Flow cytometry analysis of B cell expression of markers (left and middle panel sets), as indicated, and proliferation (right panel set) in MRL/*Fas*$^{lpr/lpr}$ mice, as in (**A**).

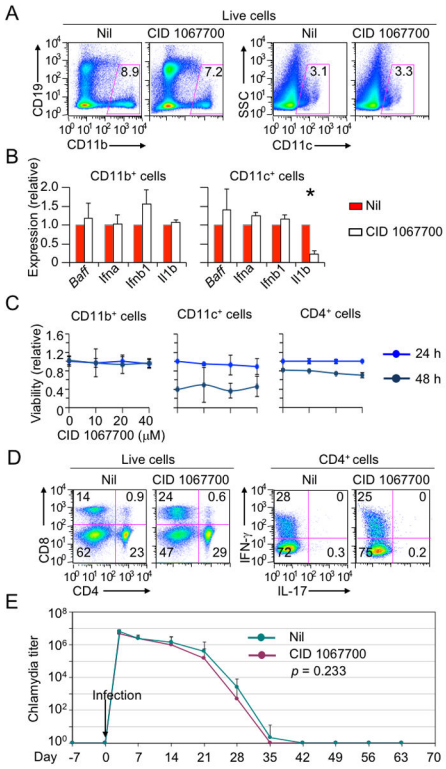

FIGURE 7.

Rab7 inhibition does not affect myeloid cells or T cells. (**A**) Flow cytometry analysis of CD11b$^+$ and CD11c$^+$ cells in 17-week old nil- or CID 1067700-treated MRL/*Fas*$^{lpr/lpr}$ mice. (**B**) Expression of cytokine-encoding genes, as indicated, in CD11b$^+$ and CD11c$^+$ cells generated from the bone marrow cells isolated from untreated 10-week old MRL/*Fas*$^{lpr/lpr}$ mice and then stimulated by CpG ODN *in vitro* in the presence of nil or CID 1067700 (mean and s.d. of triplicate samples; *, $p < 0.05$). (**C**) Survival of CD11b$^+$ and CD11c$^+$ myeloid cells as well as CD4$^+$ T cells isolated from untreated 10-week old MRL/*Fas*$^{lpr/lpr}$ mice and cultured *in vitro* in the presence of nil or different doses of CID 1067700 for 24 h or 48 h (mean and s.d. of triplicate samples). (**D**) Flow cytometry analysis of proportion of CD4$^+$ T cells and expression of IFN-γ in CD4$^+$ T cells in nil- or CID 1067700-treated MRL/*Fas*$^{lpr/lpr}$ mice, as in (**A**). Expression of IL-17 is low despite the important role of this cytokine in lupus (70). Consistent with reduced splenomegaly, the number of T cells was reduced, possibly as the secondary effect of reduced activity of autoreactive B cells. No CD19$^+$ cells expressed IFN-γ or IL-17 (not shown). (**E**) Shedding of chlamydia in C57 mice treated with nil or CID 1067700 (mean and s.e.m. of 5 mice in each group). B cells are not required for the clearance of primary chlamydia infection. (**A, C, D**), representative of three independent experiments.

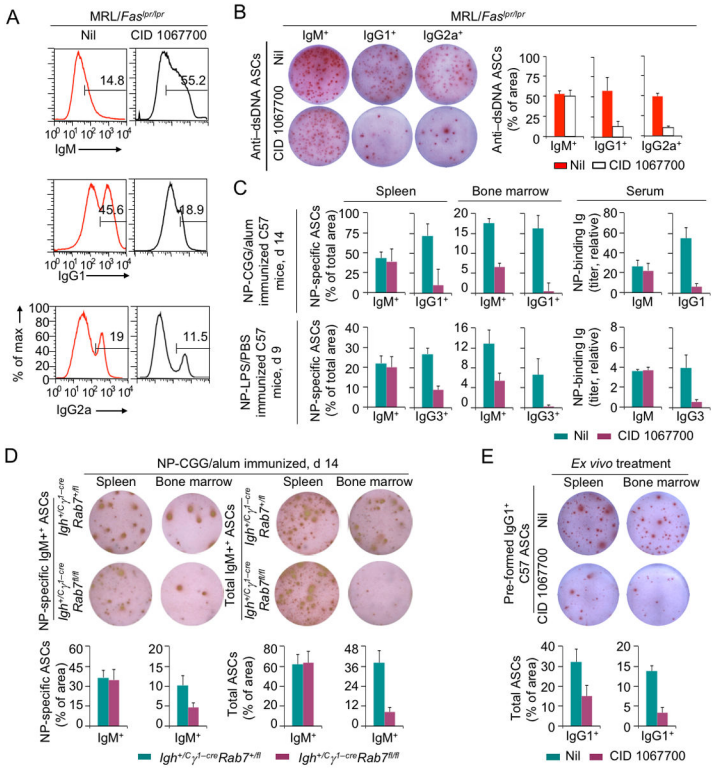

FIGURE 8.

Rab7 deficiency or inhibition impairs ASC production/functions *in vivo* and *in vitro*. (**A**) Levels of intracellular IgM, IgG1 and IgG2a in spleen CD138^{+} cells from 17-week old nil- or CID 1067700-treated MRL/*Fas*$^{lpr/lpr}$ mice (representative of three independent experiments). (**B**) ELISPOT analysis of IgM^{+}, IgG1^{+} and IgG2a^{+} ASCs in 17-week old nil- or CID 1067700-treated MRL/*Fas*$^{lpr/lpr}$ mice (right panels, mean and s.e.m. of four pairs of mice). (**C**) ELISPOT analysis of IgM^{+} and IgG^{+} (IgG1 or IgG3, as indicated) NP-binding ASCs in the spleen and bone marrow, as well as titers of circulating NP-binding IgM and IgG1 or IgG3 Abs, in nil- or CID 1067700-treated C57 mice immunized with NP-CGG (top panels) or NP-LPS (bottom panels). (mean and s.e.m. of three pairs of mice). (**D**) ELISPOT analysis of IgM^{+} NP-binding and total ASCs in the spleen and bone marrow in *Igh*$^{+/C\gamma 1\text{-}cre}$*Rab7*$^{fl/fl}$ mice and their *Igh*$^{+/C\gamma 1\text{-}cre}$*Rab7*$^{+/fl}$ littermates immunized with NP-CGG (mean and s.e.m. of three pairs of mice). (**E**) ELISPOT analysis of IgG1^{+} ASCs isolated form the bone marrow of C57 mice and treated *in vitro* with nil or CID 1067700n for 24 h before incubation for 24 h in the presence of nil or CID 1067700, totaling 48 h treatment (mean and s.e.m. of three independent experiments).

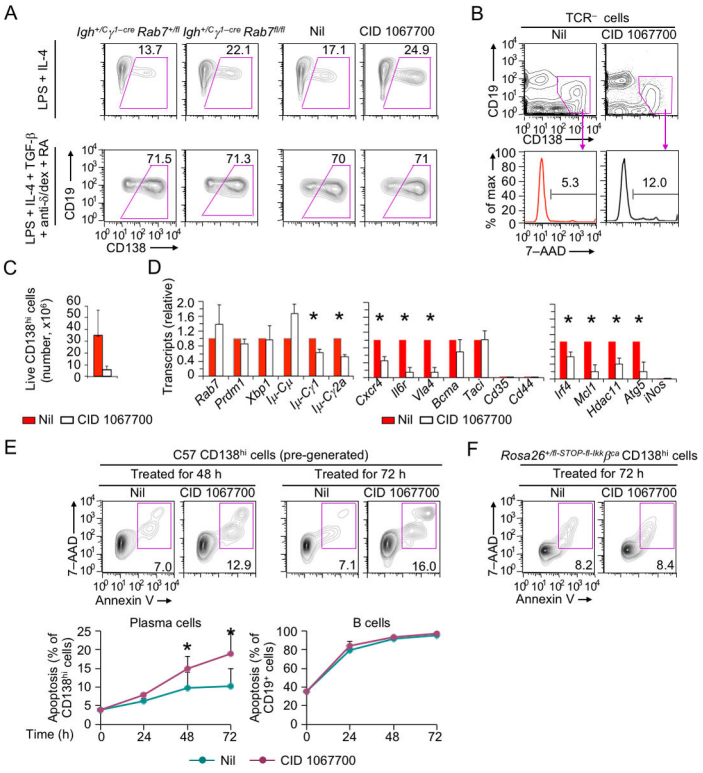

FIGURE 9.

Rab7 deficiency or inhibition impairs the survival of plasma cells, but not their generation. (**A**) Generation of CD19$^{-/lo}$CD138^{hi} plasma cells *in vitro* from *Igh*$^{+/C\gamma 1\text{-}cre}$*Rab7*$^{fl/fl}$ B cells and their *Igh*$^{+/C\gamma 1\text{-}cre}$*Rab7*$^{+/fl}$ B cell counterparts upon stimulation by LPS plus IL-4 or IL-4, TGF-β, anti–δ/dex and RA (left panels) as well as from C57 B cells undergoing same stimulation and treated with nil or CID 1067700 (right panels). (**B**) Flow cytometry analysis of total (TCR^{-} CD19$^{-/lo}$)CD138^{hi} cells in 17-week old nil- or CID107700-treated MRL/*Fas*$^{lpr/lpr}$ mice (top panels) and proportion of dead (7–AAD^{+}) cells (bottom panels). The proportion of (TCR^{-}CD19^{+}CD138^{-}) B cells was increased, but their number and viability were not changed (data not shown). Representative of three independent experiments. (**C**) Flow cytometry analysis of the number of live (TCR^{-}CD19$^{-/lo}$)CD138^{hi} cells in MRL/*Fas*$^{lpr/lpr}$ mice, as in (**B**, mean and s.d. of four pairs of mice). (**D**) Expression of different transcripts, as indicated, in live 7–AAD^{-}CD138^{hi} cells sorted from 17-week old nil- or CID 1067700-treated MRL/*Fas*$^{lpr/lpr}$ mice. Like *Cd35* and *Cd44* (which do not promote plasma cell survival), *Vla4* and *Cxcr4* are also involved in plasma cell homing to the bone marrow. Expression of *iNos,* as suggested to promote plasma cell survival in normal mice, was not detectable. Decreased expression of Iμ-Cγ1 and Iμ-Cγ2a in plasma cells was expected, due to reduced CSR. Data were depicted as the ratio of values in CID 1067700-treated mice to those in nil-treated mice (mean and s.d. of four pairs of mice; *, $p < 0.05$). (**E**) Flow cytometry analysis of early (Annexin V^{+} 7–AAD^{-}) and late (Annexin V^{Hi} 7–AAD^{+}) apoptosis in pre-generated CD19$^{-/lo}$CD138^{hi} plasma cells (after stimulation by LPS plus IL-4, IL-5, TGF-β, anti–δ/dex and RA for 66 h) after treatment with nil or CID 1067700 for 24 h, 48 h and 72 h (the histogram depicts the mean and s.e.m. of three independent

experiments; death of residual $CD19^{+}$ B cells in the same culture was not affected by CID 1067700). Flow cytometry data (top panels) are representative of three independent experiments. (**F**) Survival of $CD19^{-/lo}CD138^{hi}$ plasma cells pre-generated in the presence of pMIG-*Cre* retrovirus to express $IKK\beta^{CA}$ and then treated with nil or CID 1067700 for 72 h. Representative of three independent experiments.